國立臺灣大學生醫電子與資訊學研究所

碩士論文

Graduate Institute of Biomedical Electronics and Bioinformatics

College of Electronic Engineering and Computer Science

National Taiwan University

Master Thesis

果蠅發育過程動態生物網路功能性模組之特性分析研究

Integrative Network Analysis Reveals Dynamic Functional

Modules in *Drosophila melanogaster* Embryonic Development

研究生:吳聿笙（Yu-Sheng Wu）

指導教授：阮雪芬 博士 (Hsueh-Fen Juan)

黃宣誠 博士 (Hsuan-Cheng Huang)

歐陽彥正 博士 (Yen-Jen Oyang)

中華民國 99 年 7 月

July, 2010

國立臺灣大學碩士學位論文
口試委員會審定書

果蠅發育過程動態生物網路功能性模組之特性

分析研究

Integrative Network Analysis Reveals Dynamic

Functional Modules in *Drosophila melanogaster*

Embryonic Development

本論文係吳聿笙君（R97945039）在國立臺灣大學生醫
電子與資訊學研究所完成之碩士學位論文，於民國九十九年
七月一日承下列考試委員審查通過及口試及格，特此證明

口試委員：（指導教授）

系主任、所長

誌 謝

中文摘要

胚胎發育是一門已被廣泛研究的學門。然而，發育過程中蛋白質交互作用網路的動態變化卻很少討論到。分子網路是主導分子作用機制的骨幹，結合基因表現數據與蛋白質網路的結合可以幫助我們更了解疾病的分子機制。蛋白質交互作用建構出來的是一個靜態的網絡；結合不同特定生物環境下的基因表現量資料，可以進一步得到動態特性的資訊。在這個研究中，我們提出了一個整合性的網路分析方法。將基因表現量的資訊結合蛋白質交互作用網路及生物功能的註解資料，我們找出主導發育過程中的分子模組。藉由時間序列的基因表現量資訊與果蠅蛋白質網路的整合分析，我們找到不同發育時期的 co-expressed 蛋白質網路。結合生物功能註解及動態網路的資訊，藉由統計方法，我們找出各時期的功能性模組。且分析其扮演角色及在不同發育時期表現量上的動態變化。總結，此研究增加了我們對果蠅發育過程一些機制的了解。除此之外，更為未來研究提供了很好的素材。

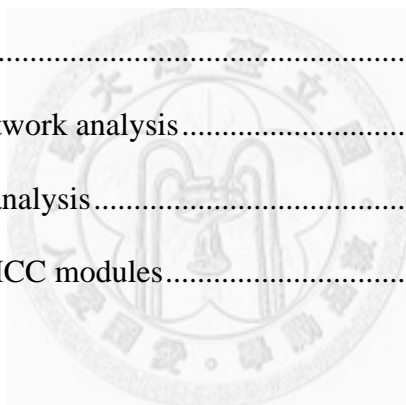關鍵字: 胚胎發育;時間序列性;共調控;蛋白質交互作用;生物網路;微陣列晶片;果蠅

ABSTRACT

Embryonic development has been extensively studied, but the dynamics of its protein-protein interaction network remains elusive. As molecular networks represent the backbone of molecular activity within cells, integrative analysis of transcriptomic profiles in the context of protein interaction networks provides opportunities for understanding the molecular mechanism of diseases. While protein-protein interaction data constitute static network maps, integration of condition-specific co-expression information provides clues to the dynamic features of the networks. Here, we present an integrative network analysis approach that integrates gene expression profiles with protein-protein interaction and biological function annotations to elucidate molecular modules during developmental processes. Integrating time-series transcriptomic profiles and protein-protein interactome of *Drosophila melanogaster*, we obtained co-expressed protein interaction networks in different developmental stages during its embryonic development. Applying enrichment analysis for functional dyads and clustering analysis based on network properties or expression profiles, we identified functional modules in each stage and investigated their roles and expression dynamics across stages. In conclusion, this study enriches our understanding of the *D. melanogaster* developmental process and provides clues for further research.

keywords: embryonic development; time-series; co-expression; protein-protein interaction; biological network; microarray; *Drosophila*

CONTENTS

LIST OF FIGURES

viii

LIST OF TABLES

Chapter 1　Introduction

In the present understanding, genome contains the blueprint and the instructions to construct an organism, and thousands of genes constitute a genome. However, most biological mechanisms are carried out through the cooperation of multiple proteins, the product of genes. Proteins play a variety of roles, including regulatory, signaling, enzymatic and structural roles. Different kinds of relations can be constructed into layers of complex biological networks, such as protein-protein interaction network, regulatory network, and metabolic pathways.

In recent years, research has increasingly focused on the study of high-throughput experiment design, and more and more high-throughput data is becoming available. The design of yeast-two-hybrid [1] and protein co-immunoprecipitation [2] techniques have benefited the construction of protein-protein interaction maps. The birth of microarray [3] and deep sequencing technologies [4] have produced thousands of large-scale expression data, and have become a common procedure in biological research. NCBI built up a platform named GEO to collect formatted expression data and corresponding raw data [5], which has promoted the prosperity of the study of expression association.

1.1   Graph theory

In computer science and mathematics, graph theory has extensively studied, and network analysis is a topic of graph theory. In 1999, Barabási and Albert found the architecture of real-world networks are governed by a few principles. The most important principle is that the degree distributions of networks in nature mostly follow a power law, which means most nodes have only a few links and a few nodes with very large number of links, and the kind of networks are called complex networks. Comparing with random network, the main different feature is the coexistence of nodes of widely different degrees[6]. The finding provides a strong backbone for complex network studies.

For a graph G = (V, E) with n vertices, each vertex have different network properties, and the measurement of network properties help us understand the role of different vertices in a network. In the following, we introduce several significant network properties below:

(1) **Degree** :

$$D(v) = \left| \{e_{vw}\}_{w \in V \setminus v, e_{vw} \in E} \right|$$

Degree is defined as the number of direct edges linked to a vertex *v*.

(2) **Betweenness**:

$$B(v) = \sum_{s \neq v \neq t \in V} \frac{\sigma_{st}(v)}{\sigma_{st}},$$

The parameter σ_{st} is the number of shortest path from vertex s to t, and $\sigma_{st}(v)$ is the number of shortest path passing through v from s to t.

Betweenness is defined as the percentage of shortest paths passing through a vertex *v*.

(3) **Closeness**:

$$C(v) = \frac{1}{\sum_{t\in V\backslash v} d_G(v,t)},$$

The function $d_G(v,t)$ is the geodesic distance between vertex v and t.

Closeness is defined as the average geodesic distance between a vertex *v* and all other vertices.

(4) **Clustering coefficient**:

$$CC(v) = \frac{|\{e_{v_i v_j}\}|}{k_i(k_i-1)/2} : v_{i,}v_j \in V_v, e_{v_i v_j} \in E$$

Clustering coefficient is defined as the percentage of the neighboring vertices connecting to each others.

1.2 Embryonic development of *Drosophila melanogaster*

Animal development starts with fertilization, and goes into the process of embryogenesis by which a fertilized egg develops into a fetus. In general, embryonic development has four significant stages, including cleavage, blastulation, gastrulation, and organogenesis.

In the beginning, the nucleus of a fertilized egg starts cleavage, and the process occurs over thirteen cycles. In the ninth cycle, the nuclei migrate towards the periphery of the egg [7]. In the thirteenth cycle, each nucleus forms into an individual epithelial cell, and phases into the stage of cellular blastoderm. Upon the completion of blastulation, the cells starts to move, and form into different germ layers, including ectoderm, mesoderm and endoderm [8], followed by the three germ layers developing into different types of organs. The ectoderm develops into the nervous system and integument. The mesoderm develops into muscles, bones and connective tissues. The endoderm develops into the respiratory system, endocrine glands and inner organs. Fig. 1-1shows the stages of *Drosophila* development.
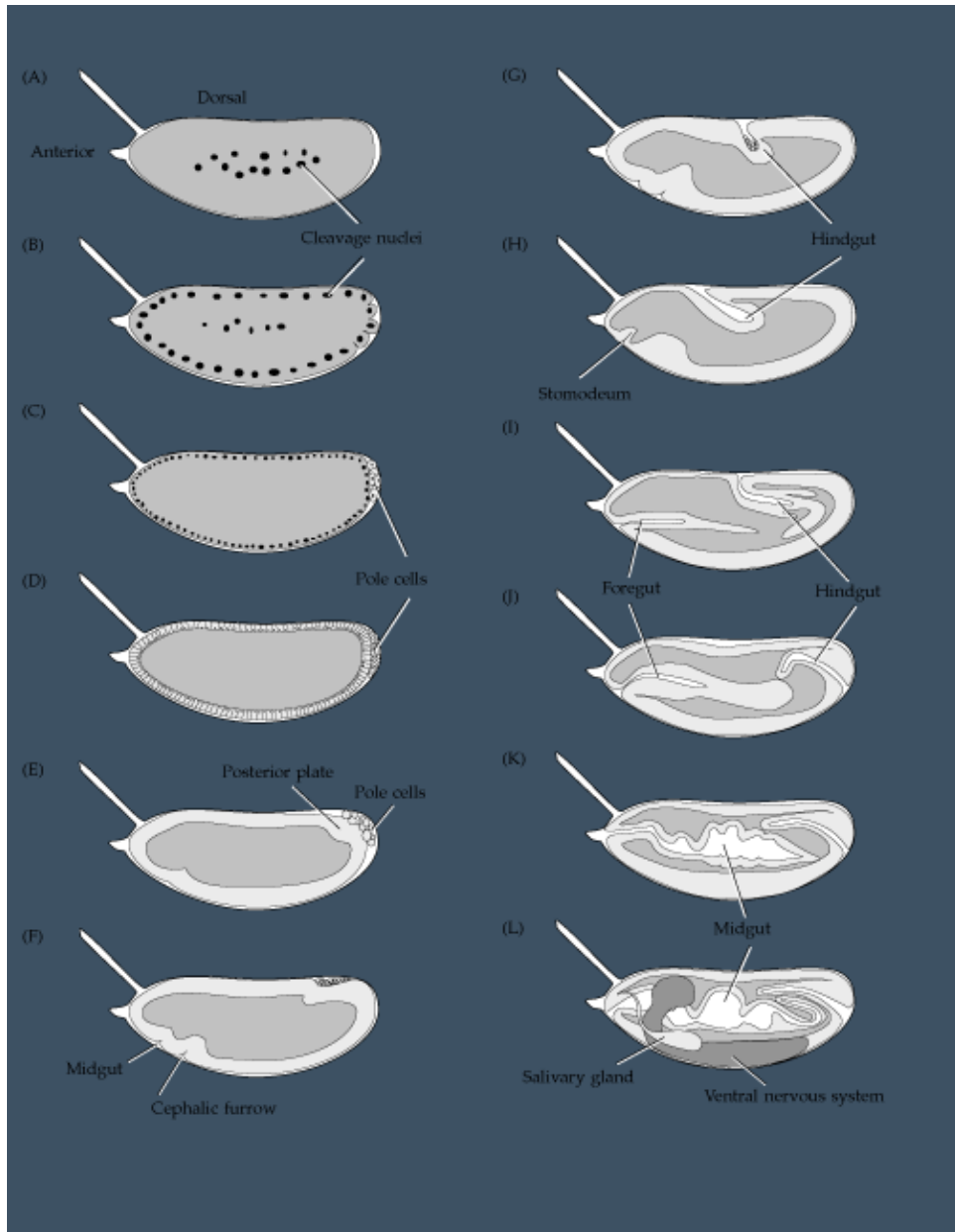
Fig. 1-1   Stages in embryonic development of *Drosophila melanogster* [9]. (A) Early cleavage (B) Migration of cleavage nuclei (C) Formation of syncytial blastoderm (D) Cellular blastoderm (E) Early gastrulation (F) Midgut invagination (G) Germ band extension (I) Stomodeal invagination (J) Shorten embryo (K) Dorsal closure (L) Condensation of ventral nervous system.

1.3 Aims

Embryonic development has been extensively studied, but the dynamics of its protein-protein interaction network remain elusive. Integrating time-series expression data and protein-protein interaction networks, we attempted to design a method of analyzing the dynamics during *Drosophila* embryonic development.

The von Baer's laws arose from the observation of visible characteristics. However, whether the concept is valid on a molecular level has never been shown. Combining time-series expression data and data from protein-protein interaction networks, we have designed a method to model the modularity structure of networks. Furthermore, we desired to explain the relation between time during development and generality of characteristics.

Chapter 2   Material and methods

2.1   Developmental dynamic network construction

2.1.1   Protein-protein interaction data

The protein-protein interaction data were acquired from DroID database[10], and only the physical interactions were used, not the predicted ones. 7,666 proteins and 25,793 interactions were used to construct the PPIN, not including self-loop interactions.

2.1.2   *D. melanogaster* life-cycle time-series expression data

The time-series data were obtained from the flybase website[11], and covered four major fly developmental stages, including 30 time-points over embryo development, 10 time-points over larval development, 18 time-points over metamorphosis, and 4 time-points each for male and female adult flies. The platform spotted amplicons covered 85% of the *D. melanogaster* genes, and amplicons were mapped to *D. melanogaster* assembly and annotation version 5.10. The study focused on the active mechanism during embryo development. Therefore, we only used the embryonic part of the expression data.

The reference set consisted of pooled RNA samples across all time-points in the following ratio (6 : 2.5 : 3.5 : 1) to (embryo : larva : metamorphosis : adult), based on the analysis of poly A+ RNA from each stage.

2.1.3 Flowchart

First, applying the time-series expression data of *Drosophila* development to calculate the correlation between every PIN, we constructed the dynamic network, which we called the co-expressed network. Second, we subdivided the co-expressed network into functional modules. Finally, the regulation of functional modules has different transition stages. In our hypothesis, the members of a functional module have higher correlation level in the transition stages. Therefore, we filtered the median of moving correlation coefficient (MCC, details in section 2.1.7) to select the significant active stages, and the median came from the median of MCC between every interaction in a functional module.
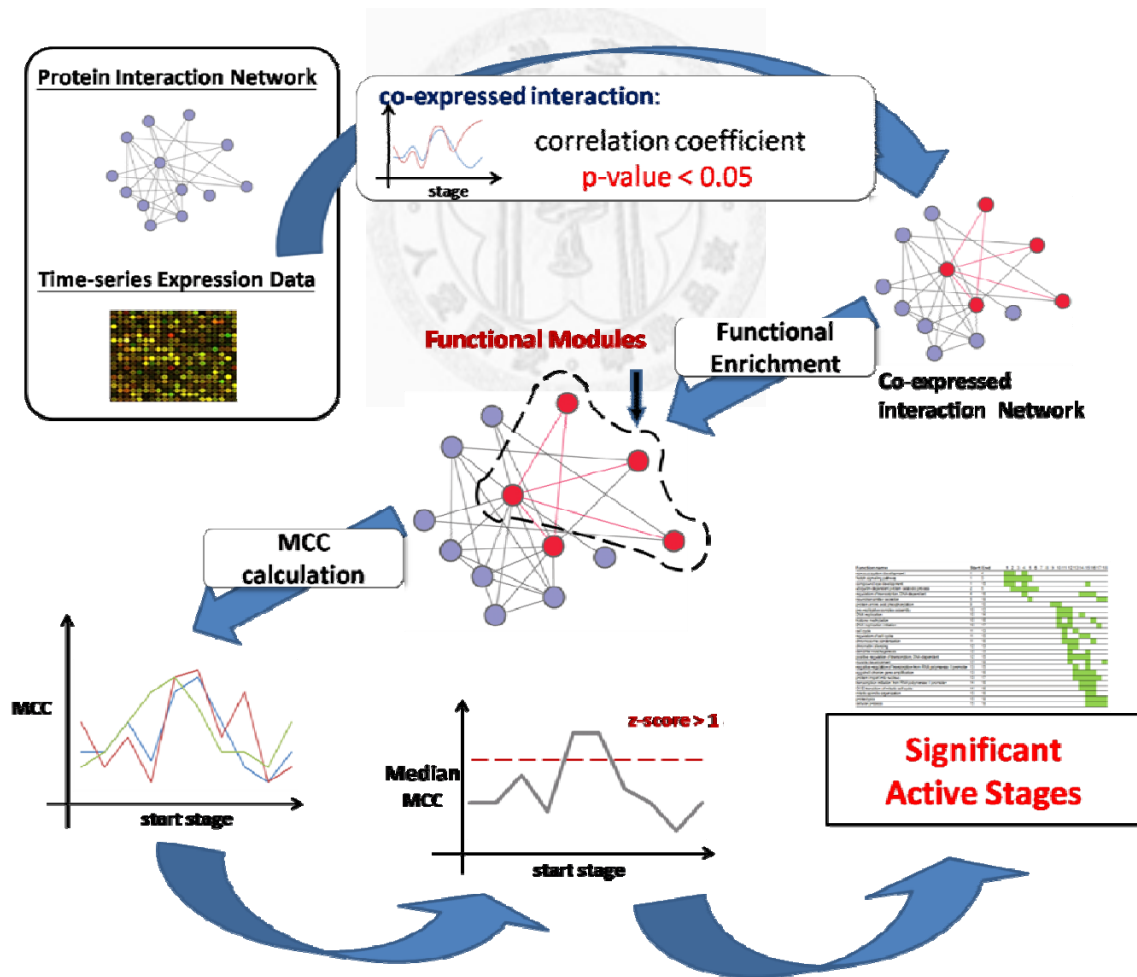
Fig. 2-1 Flowchart of developmental functional co-expressed network construction.

There are 4 steps in the flowchart. Step 1, we constructed the developmental co-expressed network by similarity of expression profile, and then extracted the functions with significant statistical enrichment. Step 3, we calculated the moving correlation coefficient profile of interactions in modules, and picked relative high positions of median profile to be the active stages.

2.1.4 Co-expressed network construction

To elucidate the dynamic developmental situation on the level of protein-protein interaction network, we applied the co-expression level to explain the strength of interactions. The co-expressed network collected the interactions with significant correlation (Fig. 2-2). Moreover, the co-expression analysis can reduce the false-positive ratio.
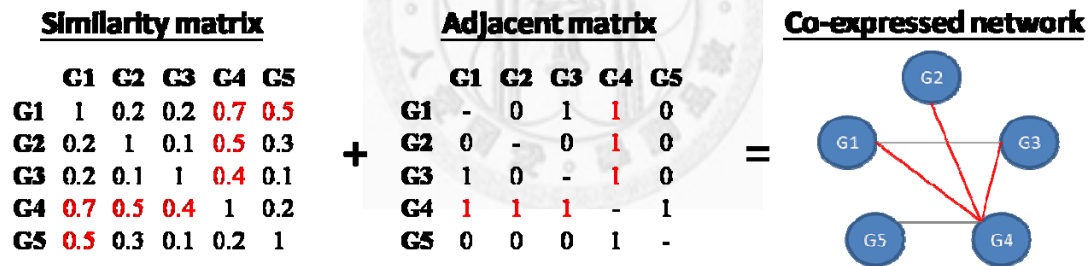
Fig. 2-2 Construction of co-expressed network. G1 to G5 are gene identifiers, and an array represents all possible interactions between genes. Similarity matrix stores the values of correlation. Adjacent matrix stores the relations of protein-protein interaction in a binary form.

2.1.5 Gene ontology information

The gene ontology consortium has systematically defined the biological terms in a hierarchical structure, categorizing the terms into three major domains: (1) biological

processes, (2) cellular components, (3) and molecular functions. Another useful source is the collections of species-specific function information, called species association file. For the functional analysis, we retrieved the gene ontology and the association file of *Drosophila*.

The number of genes defined in the association file was 10115 in the biological process domain, 8448 in the cellular component and 10958 in the molecular function domain. The number of functional dyads, which are defined as two genes having the same function in one connection, was 3196 in the biological process domain, 5971 in the cellular component domain and 4394 in the molecular function domain.

2.1.6   Functional module extraction

In network biology, a functional module refers to the subnetwork corresponding to a biological unit, and   the corresponding mechanism is hard to understand as isolated components [12]. In previous studies, two main problems arise. First, most algorithms only detected strongly-connected components. Therefore, the basic criterion resulted in an overall low coverage rate. Second, most methods ignored cases in which modules overlap. Most current methods were designed by the parition algorithm, which means each protein can only be contained in a specific paritional module [13].

We used the functions defined by gene ontology (details in 2.1.5) and estimated their significance by hypergeometric test. The testing procedure is as below:

input:
@Original_network (N,EN), @Sub_network (X, EX)
output:

```
for each @function in gene ontology definition:
    @FO(n,en) = SubNetworkOfTheFunction( @Original_network, @function )
    @FS(x, ex) = SubNetworkOfTheFunction( @Sub_network, @function )
    @significant = False
    if hypergeometric_test( N, X, n, x ) then
        if hypergeometric_test( EN, EX, en, ex ) then
            @significant = True
        end if
    end if
    if @significant == True:
        @SignificantFunctionalModules.push(FS)
end for
return @SignificantFunctionalModules
```

In the construction of functional co-expressed network, the sub-network is the co-expressed network, and both the original network and co-expressed network themselves are also composed of many functional sub-networks. The procedure iteratively checked the significance of the functions and picked out the significant functional sub-networks. The union of significant functional modules is called "functional co-expressed network".

2.1.7 Moving correlation coefficient

The number of samples determines accuracy of correlation measure. The general time-series data have only a few replicates per time point. Therefore, we applied a method, called moving correlation coefficient, both to preserve accuracy and to obtain as much data as possible. In this method,"moving" reflects that the measurement accepts overlapping. For instance, a time-series data have 1 to n time points. Therefore, the maximum number of measurements is n/6 without overlapping, and n-6 with overlapping.

2.1.8 Module relational network

To elucidate the interwoven relation between modules, we provided a method to reconstruct the relations between modules under different conditions. We transformed the modules into nodes, and the edges represented the overlap that occurs between two modules (Fig. 2-3).
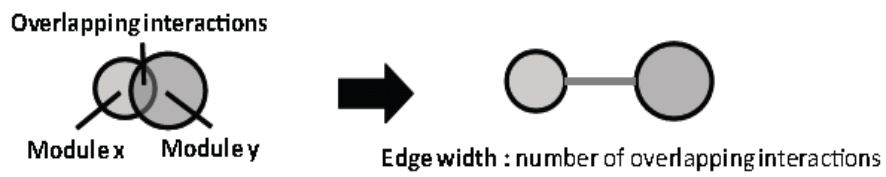
Fig. 2-3 Transformation procedure of functional co-expressed network into module relational network

2.2   Construction of moving co-expressed networks

The method was designed for the purpose of seeing more detailed functions in different stages. In the flowchart in Fig. 2-1, we used the entire microarray data set, and intended to retrieve the most general functions for the entire development processing.

Therefore, we modified the previous flowchart and reintroduced the "moving" concept (in 2.1.7), which means the splicing of the microarray with maximum overlapping. Additionally, the method was designed to have a fixed window. Because of the requirement of correlation calculation, it is better if the the window size is larger than 6.

The procedure has only two steps, setting up a window size to splice the time-series data and constructing the co-expressed networks (Fig. 3-1).
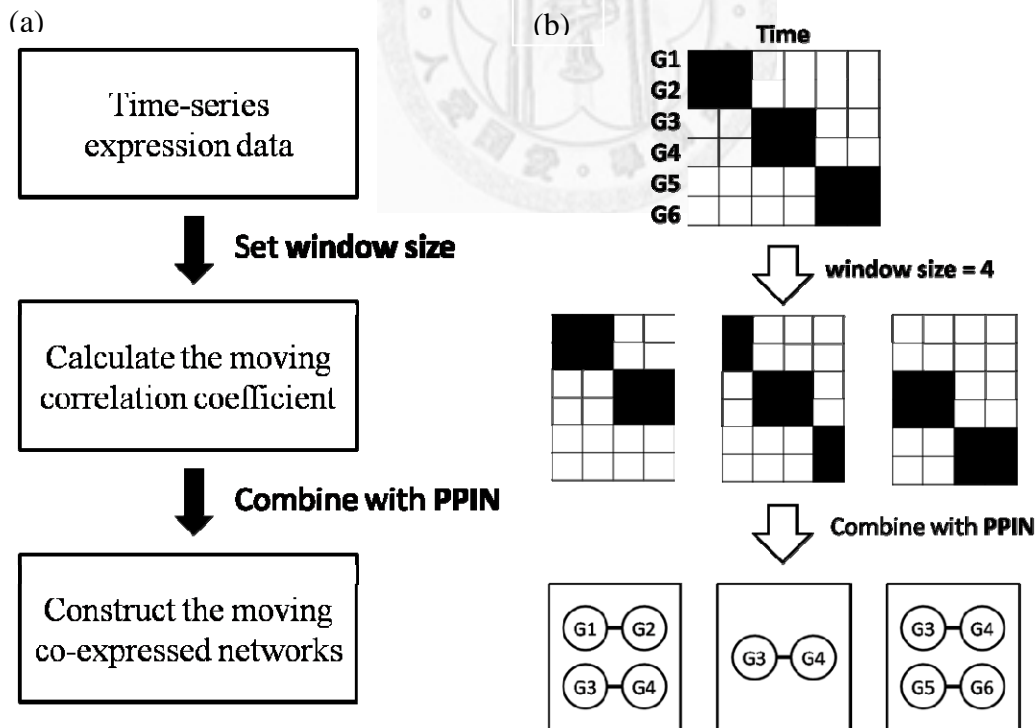
Fig. 2-4 Construction of moving co-expressed network. (a) Flowchart of moving co-expressed network construction (b) A simplified example

13

Data analysis

2.2.1 SCC distribution

In a population, the random condition often forms into a bell-shaped normal distribution, and different patterns of distribution represent that certain attributes existed. In our condition, we usually used the method to explore the attributes in different situations. In detail, we computed all pairs of genes in a microarray data, and the distribution mostly tended toward a normal distribution. In diverse conditions, different interactions participate in the working, and we compute different sets of permutations to form a SCC distribution. This method helps us to see the trends that differ from normal situation.
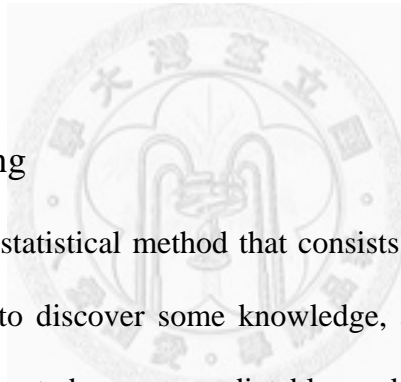
2.2.2 Random sampling

Sampling is a kind of statistical method that consists of the selection of unbiased subsets from a population to discover some knowledge, and random sampling is the method of choosing the subsets by an unpredictable random algorithm. From random samples, we can calculate estimates like mean and standard error and determine the confidence intervals.

Chapter 3   Results

3.1   Developmental functional co-expressed network

We constructed the co-expressed network (Fig. 3-1(a)) over the entire *Drosophila* embryonic development, and extracted the significantly enriched functional modules. The modules included the essential biological and developmental functions (Fig 3-3, details in Table 3.2), and were further represented in the module relation network form (Fig. 3-4). The following analysis focuses on the biological process domain (The results of other domains put in the Appendix A).

Additionally, the distribution of the spearman correlation coefficient of all protein-protein interactions is called "SCC distribution". The right-skewed SCC distribution (Fig. 3-1(b)) showed the overall higher correlation between protein-protein interactions, and implied the combination of PPIN and correlation values raised the ratio of true-positive.

(a)   (b)
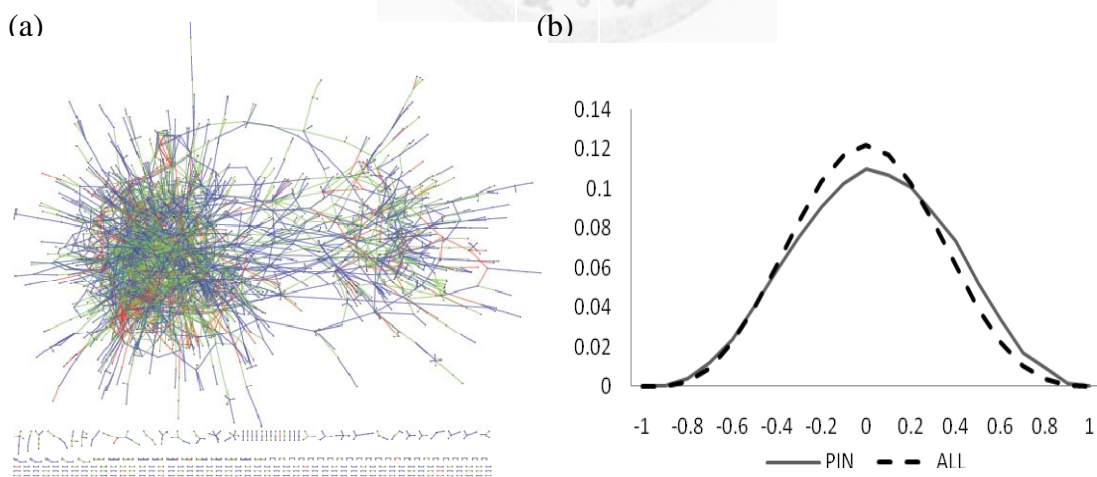
Fig. 3-1   Developmental co-expressed network and SCC distribution comparison (a) Co-expressed network; red, green, and blue bar represented high, middle, and low correlation respectively. (b) SCC distribution. Solid and dashed lines represent the SCC

distribution of PIN (protein interaction network) and the every possible combination of all genes, respectively.
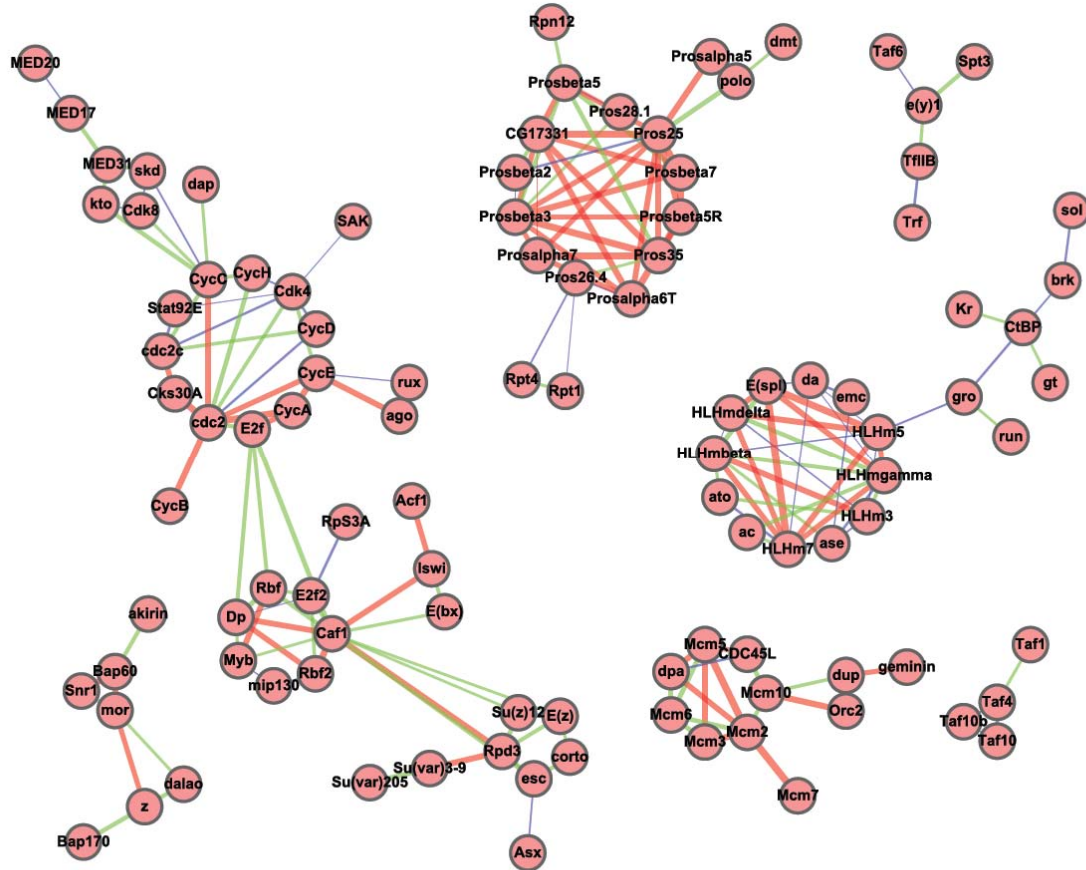
Fig. 3-2 Connected components (node number ≥ 4) of developmental functional co-expressed network, including 7 components. Red, green and blue lines represent high-correlated, middle-correlated and low-correlated interactions.
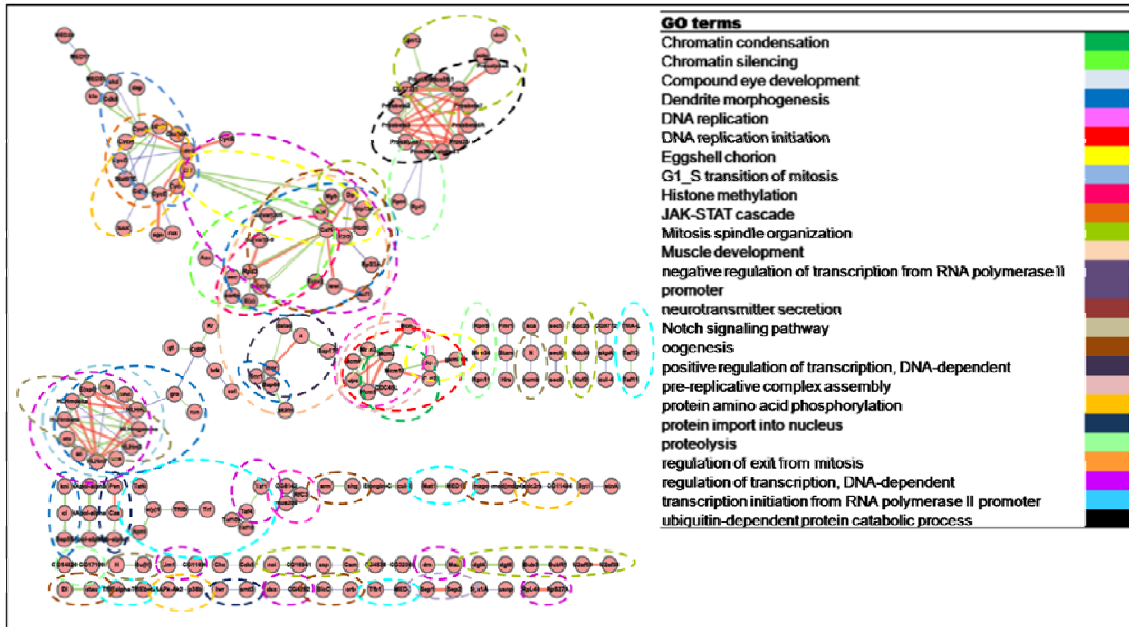
Fig. 3-3 Developmental functional co-expressed network in biological process domain. The graph only marked the go terms above level 4, including level 4. Red, green and blue edge represented high, middle and low correlation interaction respectively. The network is the union of 26 functional modules, a sub-network of PPIN. Dotted circles with the sample color contain the members of the same functional module.

Table 3.1 The functional modules and corresponding active stages.

Function name	Start	End	1	2	3	4	5	6	7	8	9	10	11	12	13	14	15	16	17	18
compound eye development	1	4	■	■	■	■														
Notch signaling pathway	1	5	■		■	■	■													
ubiquitin-dependent protein catabolic process	2	6		■	■	■	■	■												
negative regulation of transcription from RNA polymerase II promoter	2	14		■												■				
regulation of transcription, DNA-dependent	4	14				■									■	■				
protein amino acid phosphorylation	7	10							■		■	■								
JAK-STAT cascade	10	10										■								
protein import into nucleus	10	15										■					■			
pre-replicative complex assembly	10	16										■		■				■		
DNA replication	10	16										■	■	■	■			■		
DNA replication initiation	10	16										■		■	■			■		
histone methylation	10	16										■	■	■			■	■		
Oogenesis	10	17										■			■				■	
chromosome condensation	11	13											■	■	■					
chromatin silencing	11	14											■	■	■	■				
eggshell chorion gene amplification	11	15											■			■	■			
dendrite morphogenesis	12	15												■			■			
positive regulation of transcription, DNA-dependent	12	15												■	■	■	■			
regulation of exit from mitosis	12	16												■	■	■	■	■		
transcription initiation from RNA polymerase II promoter	12	16												■		■	■	■		
muscle development	12	18												■	■	■				■
G1/S transition of mitotic cell cycle	14	15														■	■			
mitotic spindle organization	14	16														■	■	■		
neurotransmitter secretion	16	18																■	■	■
proteolysis	17	18																	■	■
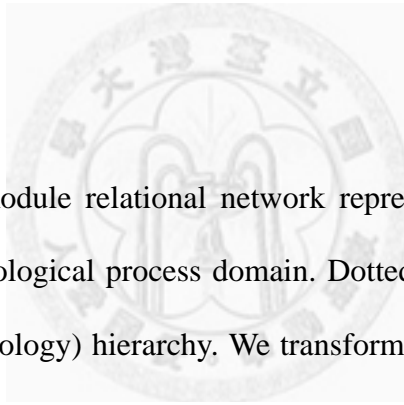
Fig. 3-4 Developmental module relational network represented the relation between inter-tangled modules in biological process domain. Dotted line represents the relation contained in GO (Gene Ontology) hierarchy. We transformed developmental functional co-expressed network (Fig. 3-3) by the method described in Section 2.1.8. A node represents a functional module, and a relation edge represents the relation of overlapping between two modules. Line width represents the number of overlapping protein-protein interaction.

Table 3.2 The functional modules of co-expressed network in biological process

domain.

Description	#Edges	P-value
ubiquitin-dependent protein catabolic process	39	5.10E-08
DNA replication initiation	12	5.84E-07
DNA replication	13	3.37E-05
pre-replicative complex assembly	8	7.20E-05
transcription initiation from RNA polymerase II promoter	23	0.00021
eggshell chorion gene amplification	11	0.00024
compound eye development	20	0.00036
muscle development	13	0.00056
histone methylation	9	0.00058
JAK-STAT cascade	6	0.00079
cellular process	14	0.00098
positive regulation of transcription, DNA-dependent	7	0.00134
Notch signaling pathway	11	0.00144
chromatin silencing	13	0.00207
dendrite morphogenesis	19	0.00258
chromosome condensation	5	0.00261
negative regulation of transcription from RNA polymerase II promoter	20	0.00304
nervous system development	17	0.00386
ATP-dependent proteolysis	10	0.00611
neurotransmitter secretion	7	0.01003
G1/S transition of mitotic cell cycle	6	0.01078
protein amino acid phosphorylation	7	0.01229
Oogenesis	7	0.01500
cell cycle	8	0.01542
regulation of transcription, DNA-dependent	21	0.01625
regulation of exit from mitosis	3	0.02836
protein import into nucleus	3	0.02836
regulation of cell cycle	7	0.03135
mitotic spindle organization	14	0.03249
Proteolysis	6	0.03920

3.2 Moving functional co-expressed network

3.2.1 Functional analysis

Following the procedure of 2.2, we set up the window size = 12 for the consideration of robustness. Therefore, 30 time points can be separated into 18 overlapping stages, and produce 18 corresponding moving co-expressed networks. Each moving co-expressed network applied the functional module extraction method (in 2.1.6). The following two lists summarize the functional modules extracted from moving co-expressed network of each stage. We separated the two lists (Table B. and Table 3.4) by the difference of active range (range = end – start). In the result, we can see detail functions.

Table 3.3 The functional modules and corresponding active stages by functional enrichment of co-expressed networks in different stages (range > 6). These modules have complex temporal patterns.

Function name	Start	End	1	2	3	4	5	6	7	8	9	10	11	12	13	14	15	16	17	18
negative regulation of transcription from RNA polymerase II promoter	1	14	■											■	■	■				
Notch signaling pathway	1	14	■	■	■	■			■	■	■		■	■		■				
compound eye development	1	17	■	■	■	■	■		■		■		■	■	■	■		■	■	
DNA replication initiation	1	18	■	■	■	■	■		■	■	■	■	■	■	■	■			■	■
ubiquitin-dependent protein catabolic process	1	18	■	■	■	■	■	■	■	■						■	■		■	■
nuclear mRNA splicing, via spliceosome	2	15		■												■	■			
transcription initiation from RNA polymerase II promoter	2	17		■									■	■		■	■	■	■	
chromosome condensation	2	18		■	■											■	■	■	■	■
pre-replicative complex assembly	2	18		■	■	■				■	■	■	■	■	■				■	■
G2/M transition of mitotic cell cycle	4	17				■					■	■	■	■	■			■	■	
cellular process	4	18				■				■	■	■					■	■	■	■
DNA replication	8	18								■	■			■	■		■		■	■
nucleosome assembly	10	17										■	■	■	■			■		
muscle development	11	18											■	■	■	■			■	
nucleosome positioning	11	18											■	■	■	■	■			■
chromatin silencing	11	18											■	■	■	■				■

Table 3.4 The functional modules and corresponding active stages by functional

enrichment of co-expressed networks in different stages (range ≤ 6).

Function name	Start	End	1	2	3	4	5	6	7	8	9	10	11	12	13	14	15	16	17	18
determination of anterior/posterior axis, embryo	1	1	■																	
regulation of pole plasm oskar mRNA localization	1	1	■																	
mitotic spindle organization	1	1	■																	
transcription from RNA polymerase II promoter	1	2	■	■																
negative regulation of transcription	1	2	■	■																
nervous system development	1	4	■			■														
regulation of transcription, DNA-dependent	4	6				■		■												
pole plasm oskar mRNA localization	6	8						■	■	■										
mesoderm development	7	7							■											
germ-line stem cell maintenance	7	11								■	■	■	■							
sensory organ precursor cell fate determination	8	9								■	■									
open tracheal system development	8	10								■	■	■								
glial cell migration	9	11									■	■	■							
centrosome organization	11	13											■	■	■					
histone methylation	11	15											■	■	■	■				
eggshell chorion gene amplification	11	16											■	■	■	■	■			
regulation of exit from mitosis	12	13												■	■					
dendrite morphogenesis	12	14												■	■	■				
neuron development	12	15												■	■	■	■			
G1/S transition of mitotic cell cycle	13	17													■	■	■	■	■	
regulation of transcription from RNA polymerase II promoter	13	17													■			■	■	
imaginal disc-derived wing vein morphogenesis	14	14														■				
positive regulation of transcription, DNA-dependent	14	16														■		■		
cell cycle	15	15															■			
sensory organ development	15	15															■			
endomitotic cell cycle	15	15															■			
positive regulation of Wnt receptor signaling pathway	15	17															■	■	■	
ganglion mother cell fate determination	15	18															■	■	■	■
actin filament organization	16	18																■		■
JNK cascade	17	17																	■	
regulation of cell shape	17	17																	■	
protein amino acid phosphorylation	17	18																	■	■
phagocytosis, engulfment	18	18																		■

3.2.2 Network properties analysis

These network properties are the average value of all genes in each moving co-expressed network, and are the values of complete *Drosophila* PPIN.

Early stages have relatively higher average degree and betweenness, and slightly lower average clustering coefficient. Average closeness has an increasing trend until the drop in the 14th stage.
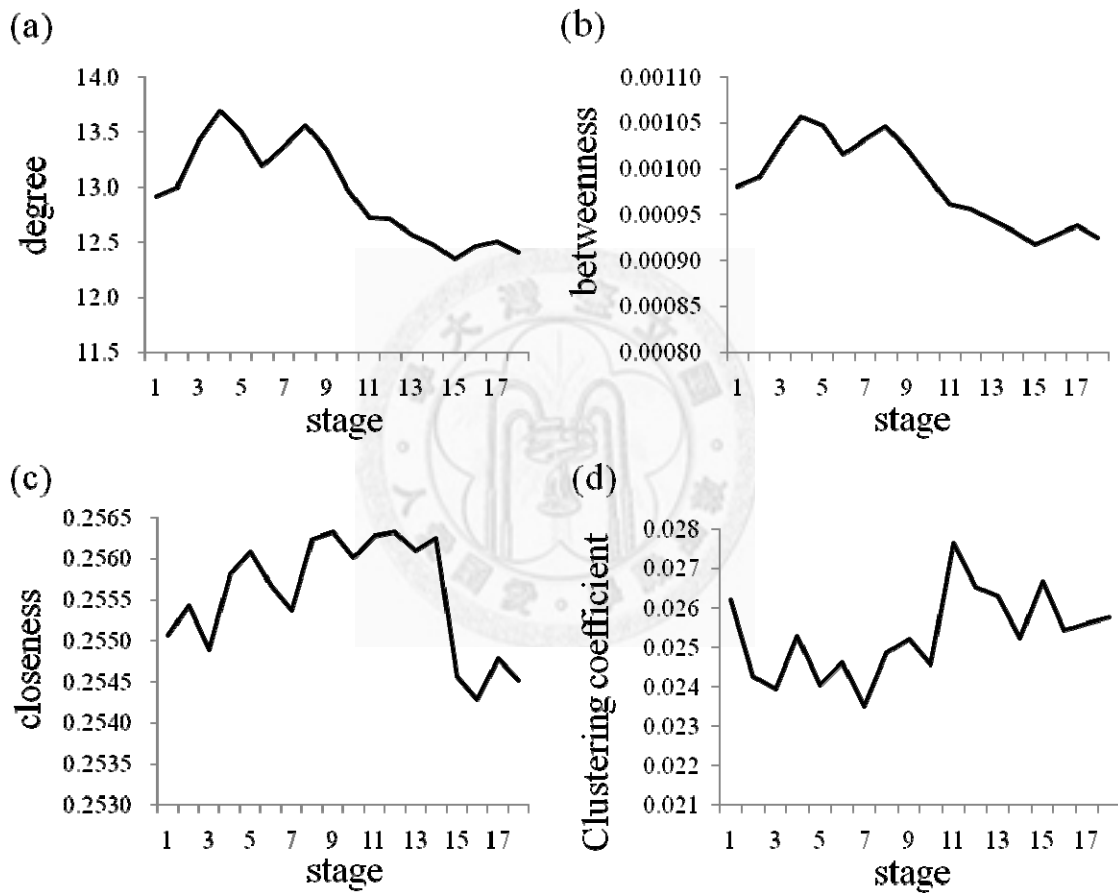
Fig. 3-5   Comparison network properties of different developmental stages (a) average degree (b) average betweenness (c) average closeness (d) average clustering coefficient.

Comparing degree distributions of different developmental stages, we found that the decreasing tendency of degree and betweenness influenced by the coverage of low-degree nodes (Fig. 3-6). In other words, co-expressed network have higher coverage of low-degree nodes in late embryonic development, and lower in early embryonic development.
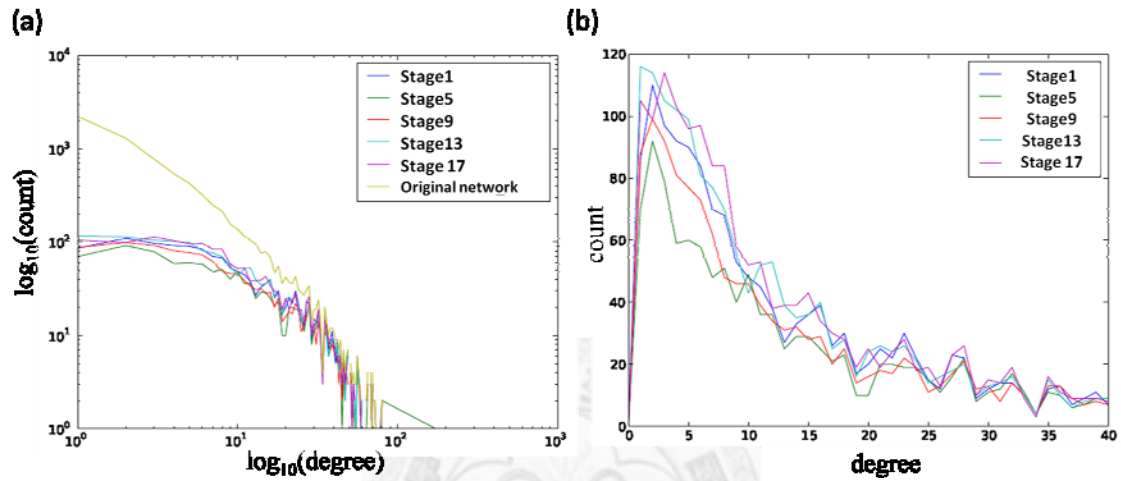
Fig. 3-6 Comparison of degree distributions of different developmental stages. (a) degree distributions with log scale (b) degree distribution. Original network represents the original PPIN. After degree bigger than 20, all degree distributions increasingly converge to a similar pattern.

Chapter 4   Discussion

We generated the active stage of modules by correlation coefficient, where the higher the correlation the higher the activity and the meaning of active stage represents the transient stages. In other words, higher deviation expression in the time duration means higher activity. Combined with expression data, the time-series expression data can be divided into several steady stages, and the steady stages with high expression may have a higher possibility to function, and vice versa.

We compared two analytic methods used in this article (Table 4.1), named co-expressed network and moving co-expressed network. The second method is obviously better than the first one. In the first method, we tried to pick active stages with relative high correlation without any statistical support, and the bias is the biggest weakness, called stage selection bias. In the second method, temporal and functional results are examined by statistical test, and detailed comparison of functional modules showed in Table 4.2. In the following, we focused on the results of second method.

Table 4.1 Comparison of two analytic methods.

	Co-expressed network	Moving co-expressed network
Gene ontology level	Lower	Higher
Parameter	No	Yes (Window size)
Specificity	Less	Flexible
Stage selection bias	Yes	No
Temporal dynamics	No	Yes

Table 4.2 Comparison the functional modules of two analytic methods. Gray and black squares represent active stages from first and second methods respectively.

Function name	Start	End	1	2	3	4	5	6	7	8	9	10	11	12	13	14	15	16	17	18

Module		
compound eye development	1	4
	1	17
Notch signaling pathway	1	5
	1	14
ubiquitin-dependent protein catabolic process	2	6
	1	18
negative regulation of transcription from RNA polymerase II promoter	2	14
	2	17
regulation of transcription, DNA-dependent	4	14
	4	6
protein amino acid phosphorylation	7	10
	17	18
pre-replicative complex assembly	10	16
	2	18
DNA replication	10	16
	8	18
DNA replication initiation	10	16
	1	18
histone methylation	10	16
	11	15
chromosome condensation	11	13
	2	18
chromatin silencing	11	14
	11	18
eggshell chorion gene amplification	11	15
	11	16
dendrite morphogenesis	12	15
	12	14
positive regulation of transcription, DNA-dependent	12	15
	14	16
regulation of exit from mitosis	12	16
	12	13
transcription initiation from RNA polymerase II promoter	12	16
	2	17
muscle development	12	18
	11	18
G1/S transition of mitotic cell cycle	14	15
	13	17
mitotic spindle organization	14	16
	1	1

During 180-195 min, embryogenesis of *Drosophila* comes to form mesoderm and endoderm layers [8]. In module of "mesoderm development", we predicted that the module activates during 180-240 min. During 260-440 min, sets of ectodermal

precursor cells cluster on both side of the 10th posterior parasegments and invaginate to form tracheal pits[14]. In module of "open tracheal system development", we predicted that the module activates during 210-330 min. In both cases, experimental and predicted results are quite identical.

In the early developmental stages, *oskar* mRNA localization plays an important role in axis determination. We discovered three related functional modules, including (1) regulation of pole plasm *oskar* mRNA localization, (2) pole plasm *oskar* mRNA localization and (3) determination of anterior posterior axis of embryo. In the modules related to *oskar*, *Mago Nashi-Tsunagi* protein complex is a member in both modules (1) and (2), and activated during 0-60 min and 150-270 min. *Mago Nashi-Tsunagi* protein complex is required to define major body axes during oogenesis of *Drosophila* [15], and without this interaction, *oskar* will fail to localize within the posterior pole plasm [15]. In our study, we found the complex also plays a role in embryogenesis. Coupled with the expression profile, we further inferred that the module is activated during 0-60 min and inactivated during 150-270 min.

The Wnt pathway is well-known for its roles in embryogenesis and cancer. During stage 15-17, we found a module related to the regulation of Wnt pathway, called "positive regulation of Wnt receptor signaling pathway". The module contains only two interactions, which are *skd-kto* and *pygo-lgs* (Fig. 4-1(a)), but successfully cover most of the members in the regulation complex of the Wnt pathway [16] (Fig. 4-1(b)).
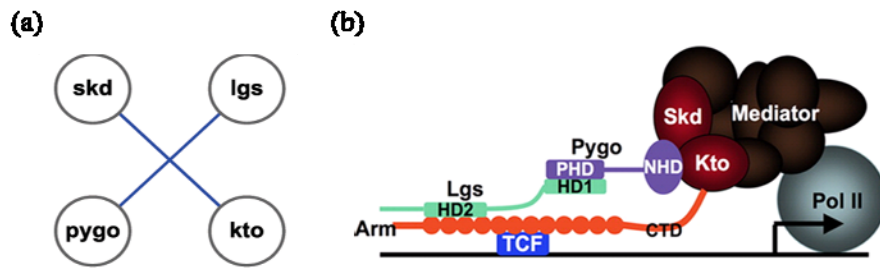
Fig. 4-1 (a) Functional module "positive regulation of Wnt receptor signaling pathway", and (b) the complex which regulates the transcription of Wnt target genes found in the study of [16]. *pygo*, *lgs*, *skd* and *kto* are the required components for the transcriptional activation of *wg* target genes.

When compared to previous studies, our method was able to produce similar results to those experimental results. Currently, temporal information on embryonic development is rather limited, mostly with a primary focus on early embryonic development. The method used in the present study provides an easier approach to obtain the temporal information of developmental processes.

Cell cycle controls the processes of cell growth and division, and the regulation of cell cycle are coordinated with developmental signaling to produce embryonic patterns [17]. Analyzing the dynamic networks from our results, the regulation circuit of cell cycle becomes more complicated from the stage 12 to stage 16. Through the comparison of network dynamics, we clearly elucidate the processing of functions at the molecular level. In previous study, they discovered that *cycC* appears to have multiple functions, such as regulation of cell cycle progression and regulation transcription by *cycC-cdk8* complex. In our study, we discovered that *cycC* also acts as a significant regulator during embryonic development.

28

Fig. 4-2   functional module "cell cycle" in different stages (window size = 12) (a) 12th stage (5.5 – 17 hours(hrs)) (b) 13th stage (6-18 hrs) (c) 14th stage (7-19 hrs) (d) 15th stage (8-20 hrs) (e) 16th stage (9-21 hrs). From the 13th stage (5.5 hrs after fertilization) on, the regulation of cell cycle becomes more and more complicated.
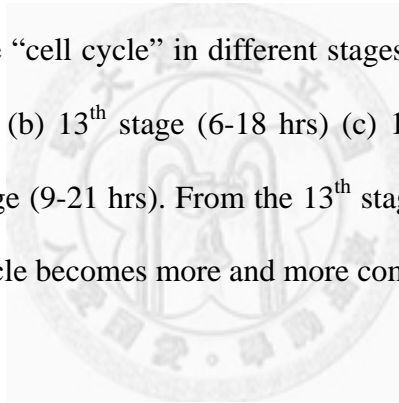
Chapter 5   Conclusion

We designed a network-based method to analyze time-series expression data in a modular view. By changing the window size, we can explore the functional modules in different time periods, trading off between robustness and specificity. A maximum window size setup can extract the most robust modules, but only for the most general functions, such as DNA replication and cell cycle regulation. An analysis setting of smaller window size provides not only more detailed functional structure but also more specific activation time points. In developmental biology, we have only limited temporal information in the scale of genomics. Our study retrieved significant active timing of functional modules, and these results can provide for further studies.

Additionally, we analyzed network properties of different developmental stages. We discovered that average degree and betweenness have a decreasing tendency and the average closeness drop in the last two stages. The tendency results from the increasing number of low-degree nodes.

REFERENCE

1. Ito, T., et al., *A comprehensive two-hybrid analysis to explore the yeast protein interactome.* Proc Natl Acad Sci U S A, 2001. **98**(8): p. 4569-74.

2. Mann, M., R.C. Hendrickson, and A. Pandey, *Analysis of proteins and proteomes by mass spectrometry.* Annu Rev Biochem, 2001. **70**: p. 437-73.

3. Schena, M., et al., *Quantitative monitoring of gene expression patterns with a complementary DNA microarray.* Science, 1995. **270**(5235): p. 467-70.

4. Margulies, M., et al., *Genome sequencing in microfabricated high-density picolitre reactors.* Nature, 2005. **437**(7057): p. 376-80.

5. Sayers, E.W., et al., *Database resources of the National Center for Biotechnology Information.* Nucleic Acids Res, 2009. **37**(Database issue): p. D5-15.

6. Barabasi, A.L. and Z.N. Oltvai, *Network biology: understanding the cell's functional organization.* Nat Rev Genet, 2004. **5**(2): p. 101-13.

7. Mazumdar, A. and M. Mazumdar, *How one becomes many: blastoderm cellularization in Drosophila melanogaster.* Bioessays, 2002. **24**(11): p. 1012-22.

8. Costa M, S.D.a.W.E., *Gastrulation in Drosophila: cellular mechanisms of morphogenetic movements.*, in *The Development of Drosophila*, M.a.M.-A. Bate, A., Editor. 1993, Cold Spring Harbor Laboratory Press: Cold Spring Harbor, NY. p. 425-466.

9. Tyler, M.S. and R.N.K. III. *DevBio.net*. 2008; Available from: http://www.developmentalbiology.net/node/44.

10. Yu, J., et al., *DroID: the Drosophila Interactions Database, a comprehensive resource for annotated gene and protein interactions.* BMC Genomics, 2008. **9**: p. 461.

11. Gauhar, Z., et al., *Drosophila melanogaster life-cycle gene expression dataset and microarray normalisation protocols.* 2008.

12. Hartwell, L.H., et al., *From molecular to modular cell biology.* Nature, 1999. **402**(6761 Suppl): p. C47-52.

13. Zhang, S., et al., *Discovering functions and revealing mechanisms at molecular level from biological networks.* Proteomics, 2007. **7**(16): p. 2856-69.

14. Manning, G.a.M.A.K., *Development of the drosophila tracheal system*, in *The Development of Drosophila*, M.a.M.-A. Bate, A., Editor. 1993, Cold Spring Harbor Laboratory Press: Cold Spring Harbor, NY. p. 609-685.

15. Mohr, S.E., S.T. Dillon, and R.E. Boswell, *The RNA-binding protein Tsunagi interacts with Mago Nashi to establish polarity and localize oskar mRNA during Drosophila oogenesis.* Genes Dev, 2001. **15**(21): p. 2886-99.

16. Carrera, I., et al., *Pygopus activates Wingless target gene transcription through the mediator complex subunits Med12 and Med13.* Proc Natl Acad Sci U S A, 2008. **105**(18): p. 6644-9.

17. Lee, L.A. and T.L. Orr-Weaver, *Regulation of cell cycles in Drosophila development: intrinsic and extrinsic cues.* Annu Rev Genet, 2003. **37**: p. 545-78.

18. Knuppel, R., et al., *TRANSFAC retrieval program: a network model database of eukaryotic transcription regulating sequences and proteins.* J Comput Biol, 1994. **1**(3): p. 191-8.

19. Halfon, M.S., S.M. Gallo, and C.M. Bergman, *REDfly 2.0: an integrated*

        database of cis-regulatory modules and transcription factor binding sites in Drosophila. Nucleic Acids Res, 2008. **36**(Database issue): p. D594-8.

20.   Tamura, K., et al., *MEGA4: Molecular Evolutionary Genetics Analysis (MEGA) software version 4.0.* Mol Biol Evol, 2007. **24**(8): p. 1596-9.

Appendix A: Regulatory network analysis

The regulatory interaction data was collected from two databases, TRANSFAC [18] and REDfly [19]. The regulatory network of *Drosophila* has 172 nodes and 293 edges. Additionally, we defined the transcription factor (TF) related to the functional modules by two kinds of relations. One is the TFs belong to the functional modules, called source TF, and another is the TFs bind to the functional modules, called regulator TF.
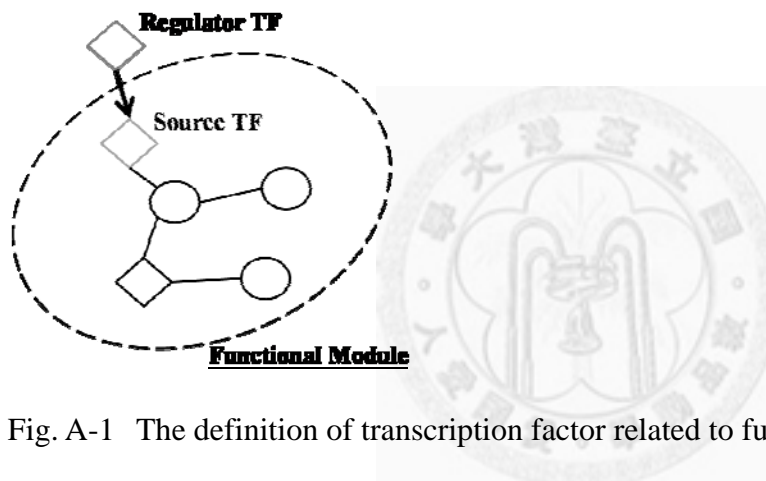
Fig. A-1 The definition of transcription factor related to functional modules

Part of the functional modules members play a role in the regulatory network (Table A.1), including compound eye development, notch signaling pathway, nervous system development, JAK-STAT cascade, regulation of transcription from RNA polymerase II promoter, egg chorion gene amplification, dendrite morphogenesis, mitosis spindle organization, and oogenesis. The connection between them is sparse, and there were only two small connected components (Fig. A-2) and many single nodes.

Combining with the regulator TFs, the connectivity increased and they are close. By the verification of random sampling test, the regulators are significantly closer than

random, with p-value < 0.005. Also, we applied the function enrichment method to the

sub-network and the result is listed below in Table A.. The SCC distribution showed that

the genes selected have a higher tendency to correlate with one another (Fig. A-).
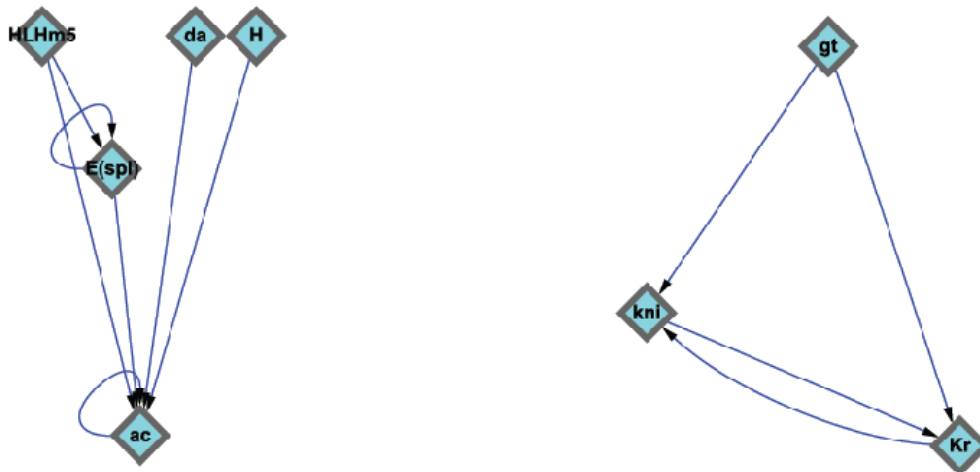
Fig. A-2 Two small connected components in the subset of regulatory network

contained source TFs.
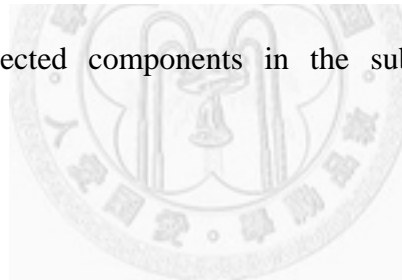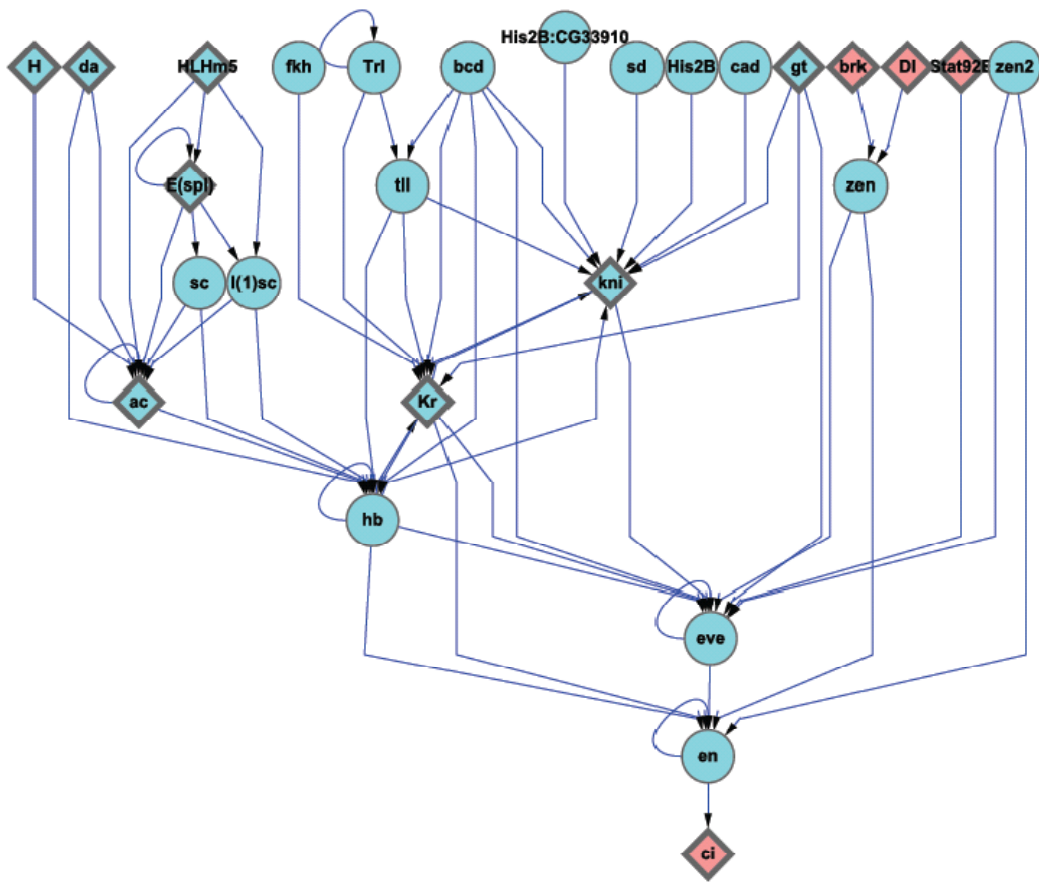
Fig. A-3 Connected component in the subset of regulatory network contained source and regulator TFs.
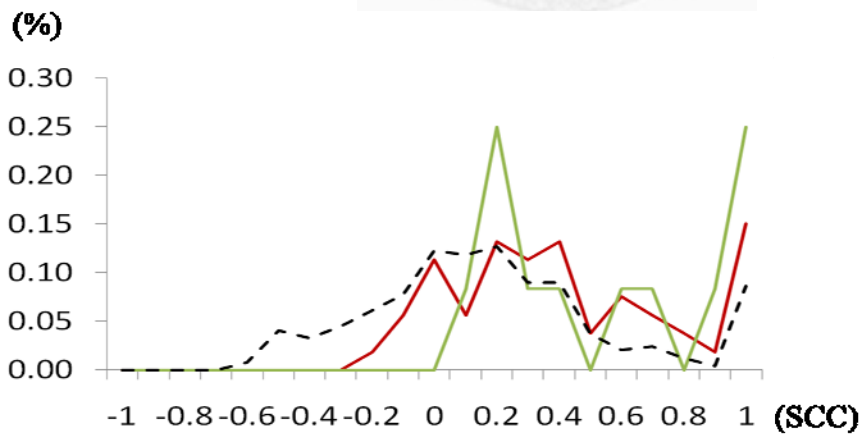
Fig. A-4 SCC distribution comparison. Dot, green and red lines are the distribution of complete regulatory network, network with source TFs and network with source and regulator TFs respectively.
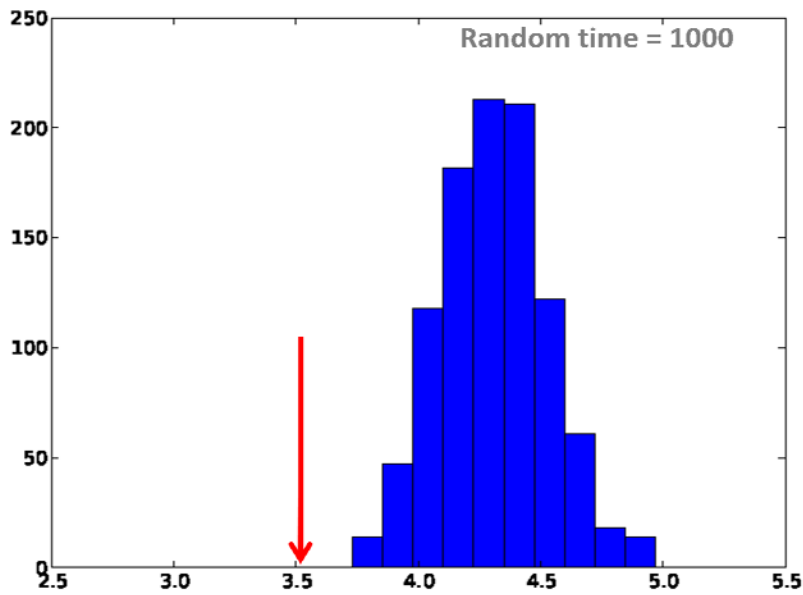
Fig. A-5 Average distance compared with random sampling distribution. Red bar

points at the average distance of

Table A.1 enrichment functions of sub-network contained source and regulator TFs

Description	#Nodes	#Edges	P-value
bristle morphogenesis	4	3	0.0159
trunk segmentation	5	12	0.0001
peripheral nervous system development	6	8	0.0001
posterior head segmentation	4	7	0.0059
central nervous system development	7	12	0.0000
ventral cord development	6	8	0.0009
nervous system development	9	6	0.0036
zygotic determination of anterior/posterior axis,	4	6	0.0002
neuroblast fate determination	6	11	0.0000
negative regulation of transcription from RNA	8	6	0.0083
positive regulation of transcription	4	5	0.0009

Table A.2 the source TFs of functional modules in biological process domain

flybase ID	gene name
FBgn0002914	Myb
FBgn0000463	Dl
FBgn0000413	da
FBgn0001150	gt
FBgn0000022	ac
FBgn0004859	ci
FBgn0000504	dsx
FBgn0001169	H
FBgn0004837	Su(H)
FBgn0001325	Kr
FBgn0010287	Trf
FBgn0000591	E(spl)
FBgn0004050	z
FBgn0001320	kni
FBgn0011766	E2f
FBgn0016917	Stat92E
FBgn0002631	HLHm5
FBgn0024250	brk

Appendix B: Evolutionary analysis

Homolog data were collected from Homologene database [5], which provides information on homologous genes among 20 completely sequenced eukaryotic genomes.
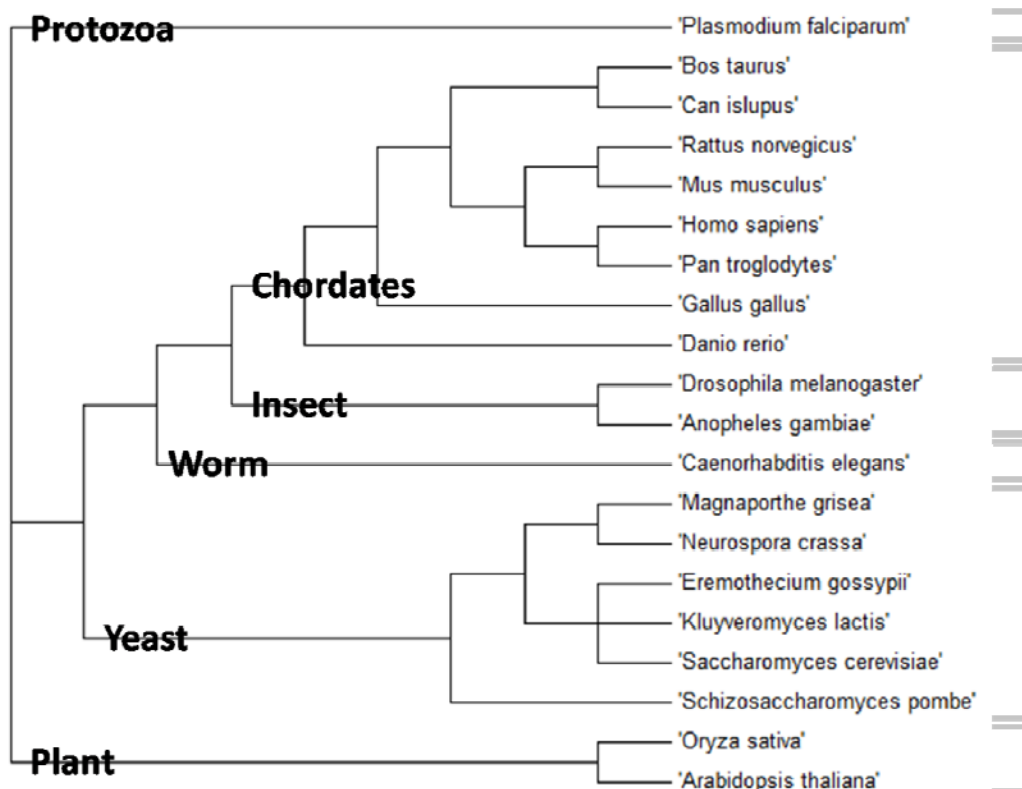
Fig. B-1 The phylogenetic tree, data retrieved from NCBI taxonomy[5], and drawn by MEGA4[20].

The conservative genes could be the ones that appeared earlier in the evolutionary history. In other words, we gave a higher score to the genes of *Drosophila* that appeared earlier. What determines appeared time depends on the phylogenetic tree, which includes 20 species from the Homologene database, with the more conservative genes having homologues in more ancient species. In the Homologene database, the 20 species are classified into 6 classes, including chordates, insects, worms, yeast, plants,

and protozoa. Because we used *Drosophila* as the model, the species of chordates will not be included in this schema, since this schema only score from a historical viewpoint. In other words, the schema can only score using species that occur earlier on in evolution compared to *Drosophila*. (Fig. 2-1)

However, the preservation of the genes in advanced species implies that there is another method of conservation. Therefore, we increased the criterion of the first schema, and gave an even higher score to the genes following the additional criterion. The second schema further clarified the stop position of evolution. (Fig. 2-1)

The conservation index of a single protein is the highest score of species contained by a homolog to the protein. The conservation index of a functional module is the average of the conservation index of all the proteins in that module.

Table B.1 schema scoring lists

	schema 1	schema 2
Insect	1	1
worm	2	2
yeast	3	3
tree	4	4
protozoa	5	5
chordates		6

Median the conservation index (cIndex) of functional module members had the cIndex of functional modules, and we had two conservation index lists of schema 1 and schema 2 (Table B.1). In the schema 2, we found that four modules have relatively low conservation indexes. Also, the four modules are the four lowest ones in the schema 2, and we supposed that they are more insect-specific than others.

We compare the correlation between conservation index and active stage (Fig. B-2), and the spearman correlation coefficient is 0.07. However, we removed the four insect-specific specific modules, and the spearman correlation coefficient is -0.58.
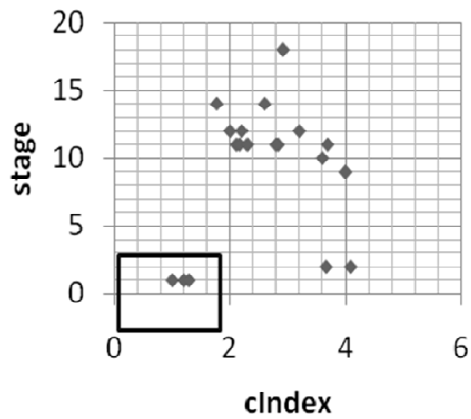
Fig. B-2 The correlation between conservation index and active stage. The three modules squared are compound eye development, nervous system development, and notch signaling pathway, insect-specific modules.

Table B.2 conservation index schema 1, the blue mark means cIndex < 2. Stage determined by z-score > 2.

function name	cIndex	stage
compound eye development	1.00	1
nervous system development	1.20	1
Notch signaling pathway	1.29	1
ATP-dependent proteolysis	4.09	2
pre-replicative complex assembly	3.67	2
ubiquitin-dependent protein catabolic process	3.60	2
DNA replication initiation	4.00	9
chromosome condensation	3.60	10
cell cycle	2.11	11
chromatin silencing	2.83	11
DNA replication	3.69	11
eggshell chorion gene amplification	2.17	11
muscle development	2.30	11
regulation of cell cycle	2.80	11
dendrite morphogenesis	2.00	12
histone methylation	3.20	12
positive regulation of transcription, DNA-dependent	2.20	12
regulation of exit from mitosis	2.67	12
negative regulation of transcription from RNA polymerase II promoter	1.77	14
protein import into nucleus	2.60	14
neurotransmitter secretion	2.92	18

Table B.3 Conservation index schema 2, the blue mark represents the functions with cIndex < 2 in the schema 1. Stage determined by z-score > 2.

function name	cIndex	stage
compound eye development	1.83	1
nervous system development	3.00	1
Notch signaling pathway	3.14	1
ATP-dependent proteolysis	5.55	2
pre-replicative complex assembly	6.00	2
ubiquitin-dependent protein catabolic process	5.75	2
DNA replication initiation	6.00	9
chromosome condensation	6.00	10
cell cycle	6.00	11
chromatin silencing	6.00	11
DNA replication	6.00	11
eggshell chorion gene amplification	6.00	11
muscle development	6.00	11
regulation of cell cycle	6.00	11
dendrite morphogenesis	4.75	12
histone methylation	6.00	12
positive regulation of transcription, DNA-dependent	6.00	12
regulation of exit from mitosis	4.67	12
negative regulation of transcription from RNA polymerase II promoter	3.31	14
protein import into nucleus	6.00	14
neurotransmitter secretion	5.67	18

Supplementary: Tables of MCC modules

Table S.1 Functional modules of MCC network in stage 1 (window size = 12).

GOID	Function name	#Edges	P-value	Edges
48749	compound eye development	12	0.00001	E(spl) pp HLHm5 , HLHm5 pp HLHmdelta , HLHmdelta pp HLHmgamma , E(spl) pp HLHmdelta , HLHm7 pp HLHmdelta , HLHm5 pp HLHmbeta , HLHm5 pp HLHm7 , E(spl) pp HLHmbeta , HLHmbeta pp HLHmdelta , svp pp toy , HLHm7 pp HLHmbeta , E(spl) pp HLHm7
6511	ubiquitin-dependent protein catabolic process	16	0.00002	Pros26.4 pp Pros35 , CG17331 pp Pros35 , Prosbeta5 pp Pros25 , Prosbeta5R pp Pros25 , Pros26.4 pp Pros25 , Prosbeta3 pp Prosbeta5R , Prosalpha7 pp Prosalpha6T , Prosbeta2 pp CG17331 , Prosalpha6T pp Prosbeta5R , CG17331 pp Pros25 , Pros28.1 pp Prosbeta5 , Prosbeta5 pp Pros35 , Prosalpha7 pp Pros35 , Prosalpha7 pp CG17331 , Prosbeta5 pp Prosbeta7 , Prosbeta3 pp CG17331
122	negative regulation of transcription from RNA polymerase II promoter	11	0.00019	E2f2 pp Rbf2 , gro pp h , CtBP pp brk , kni pp CtBP , HLHmdelta pp HLHmgamma , E(spl) pp HLHmdelta , Kr pp CtBP , kni pp ci , E(spl) pp HLHmbeta , HLHmbeta pp HLHmdelta , Caf1 pp Rbf2

6270	DNA replication initiation	5	0.00185	Mcm5 pp CDC45L , dpa pp CDC45L , Mcm2 pp Mcm7 , Mcm2 pp Mcm5 , Mcm2 pp dpa
7399	nervous system development	8	0.00322	gro pp h , da pp HLHm5 , HLHm5 pp HLHmbeta , da pp HLHmbeta , HLHm5 pp HLHmdelta , ac pp HLHmbeta , HLHmbeta pp HLHmdelta , HLHmdelta pp HLHmgamma
16481	negative regulation of transcription	5	0.00395	gro pp h , HLHm5 pp HLHmbeta , HLHm5 pp HLHmdelta , HLHmbeta pp HLHmdelta , HLHmdelta pp HLHmgamma
8595	determination of anterior/posterior axis, embryo	3	0.00949	Sos pp drk , stau pp mira , csw pp sev
6366	transcription from RNA polymerase II promoter	3	0.01522	MED4 pp MED17 , kto pp skd , RpII15 pp MED6
7317	regulation of pole plasm oskar mRNA localization	2	0.02008	stau pp mira , mago pp tsu
7052	mitotic spindle organization	6	0.03029	Pros26.4 pp Pros25 , U2af50 pp U2af38 , RpS9 pp Invadolysin , Ndc80 pp Nuf2 , Prosbeta5 pp Pros25 , Prosbeta5 pp Prosbeta7
7219	Notch signaling pathway	4	0.03308	E(spl) pp HLHmbeta , HLHmbeta pp HLHmdelta , HLHmdelta pp HLHmgamma , E(spl) pp HLHmdelta

Table S.2 Functional modules of MCC network in stage 2 (window size = 12).

GOID	Function name	#Edges	P-value	Edges
6511	ubiquitin-dependent protein catabolic process	21	4.42E-10	Prosbeta3 pp Prosbeta5 , Pros26.4 pp Pros35 , Prosalpha6T pp CG17331 , Prosbeta5R pp Pros35 , Prosbeta5 pp Pros25 , CG17331 pp Pros35 , Prosbeta5R pp Pros25 , Prosbeta3 pp Prosbeta5R , Prosalpha7 pp Prosalpha6T , Prosbeta3 pp Prosalpha6T , Prosalpha7 pp Prosbeta3 , Prosbeta2 pp CG17331 , Prosalpha6T pp Prosbeta5R , CG17331 pp Pros25 , Pros28.1 pp Prosbeta5 , Prosbeta5 pp Pros35 , Prosalpha5 pp Pros25 , Prosalpha7 pp Pros35 , Prosalpha7 pp CG17331 , Prosbeta5 pp Prosbeta7 , Prosbeta3 pp CG17331
48749	compound eye development	12	0.00000	E(spl) pp HLHm5 , HLHm5 pp HLHmdelta , HLHmdelta pp HLHmgamma , E(spl) pp HLHmdelta , HLHm7 pp HLHmdelta , HLHm5 pp HLHmbeta , HLHm5 pp HLHm7 , E(spl) pp HLHmbeta , HLHmbeta pp HLHmdelta , svp pp toy , HLHm7 pp HLHmbeta , E(spl) pp HLHm7
6270	DNA replication initiation	5	0.00107	Mcm5 pp CDC45L , Mcm5 pp Mcm3 , Mcm2 pp Mcm7 , Mcm2 pp Mcm5 , Mcm2 pp dpa
6366	transcription from RNA polymerase II promoter	3	0.01096	MED4 pp MED17 , kto pp skd , RpII15 pp MED6

16481	negative regulation of transcription	4	0.01467	HLHm5 pp HLHmbeta , HLHm5 pp HLHmdelta , HLHmbeta pp HLHmdelta , HLHmdelta pp HLHmgamma
6267	pre-replicative complex assembly	3	0.01623	Mcm5 pp Mcm3 , Mcm2 pp Mcm7 , Mcm2 pp Mcm5
6367	transcription initiation from RNA polymerase II promoter	7	0.01892	skd pp Cdk8 , TfIIEalpha pp TfIIEbeta , MED4 pp MED17 , Taf4 pp Taf10 , MED20 pp MED17 , TfIIA-L pp TfIIA-S-2 , kto pp skd
7219	Notch signaling pathway	4	0.02289	E(spl) pp HLHmbeta , HLHmbeta pp HLHmdelta , HLHmdelta pp HLHmgamma , E(spl) pp HLHmdelta
122	negative regulation of transcription from RNA polymerase II promoter	6	0.04513	kni pp ci , CtBP pp brk , E(spl) pp HLHmbeta , HLHmbeta pp HLHmdelta , HLHmdelta pp HLHmgamma , E(spl) pp HLHmdelta
30261	chromosome condensation	2	0.04529	Mcm5 pp CDC45L , Mcm2 pp Mcm5
398	nuclear mRNA splicing, via spliceosome	5	0.04911	DebB pp CG6610 , U2af50 pp U2af38 , CG6610 pp snRNP2 , Spx pp CG3605 , CG15440 pp CG1646

Table S.3 Functional modules of MCC network in stage 3 (window size = 12).

GOID	Function name	#Edges	P-value	Edges
6511	ubiquitin-dependent protein catabolic process	24	2.80E-13	Prosbeta3 pp Prosbeta5 , Pros26.4 pp Pros35 , Prosalpha6T pp CG17331 , Prosbeta5R pp Pros35 , Prosalpha6T pp Pros25 , Prosbeta5 pp Pros25 , CG17331 pp Pros35 , Prosbeta5R pp Pros25 , RpS27A pp Pros54 , Prosbeta3 pp Prosbeta5R , Prosbeta3 pp Pros35 , Prosalpha7 pp Prosalpha6T , Prosbeta3 pp Prosalpha6T , Prosalpha7 pp Prosbeta3 , Prosbeta2 pp CG17331 , Prosalpha6T pp Prosbeta5R , CG17331 pp Pros25 , Pros28.1 pp Prosbeta5 , Prosalpha5 pp Pros25 , Prosbeta5 pp Pros35 , Prosalpha7 pp Pros35 , Prosalpha7 pp CG17331 , Prosbeta5 pp Prosbeta7 , Prosbeta3 pp CG17331
48749	compound eye development	10	0.00007	E(spl) pp HLHm5 , HLHm5 pp HLHmdelta , E(spl) pp HLHmdelta , HLHm7 pp HLHmdelta , HLHm5 pp HLHmbeta , HLHm5 pp HLHm7 , E(spl) pp HLHmbeta , HLHmbeta pp HLHmdelta , HLHm7 pp HLHmbeta , E(spl) pp HLHm7
6270	DNA replication initiation	5	0.00092	Mcm5 pp Mcm6 , Mcm5 pp CDC45L , Mcm2 pp Mcm7 , Mcm2 pp Mcm5 , Mcm2 pp dpa
6267	pre-replicative complex assembly	3	0.01488	Mcm5 pp Mcm6 , Mcm2 pp Mcm7 , Mcm2 pp Mcm5

7219	Notch signaling pathway	4	0.02066	E(spl) pp HLHmbeta , numb pp N , HLHmbeta pp HLHmdelta , E(spl) pp HLHmdelta
30261	chromosome condensation	2	0.04271	Mcm5 pp CDC45L , Mcm2 pp Mcm5

Table S.4 Functional modules of MCC network in stage 4 (window size = 12).

GOID	Function name	#Edges	P-value	Edges
6511	ubiquitin-dependent protein catabolic process	21	1.11E-10	Prosbeta3 pp Prosbeta5 , Pros26.4 pp Pros35 , Prosalpha6T pp CG17331 , Prosbeta5R pp Pros35 , Prosalpha6T pp Pros25 , Prosbeta5 pp Pros25 , CG17331 pp Pros35 , Prosbeta5R pp Pros25 , Prosbeta3 pp Prosbeta5R , Prosbeta3 pp Pros35 , Prosalpha7 pp Prosalpha6T , Prosbeta3 pp Prosalpha6T , Prosalpha7 pp Prosbeta3 , Prosbeta2 pp CG17331 , Prosalpha6T pp Prosbeta5R , CG17331 pp Pros25 , Prosbeta5 pp Pros35 , Prosalpha5 pp Pros25 , Prosalpha7 pp Pros35 , Prosalpha7 pp CG17331 , Prosbeta3 pp CG17331
48749	compound eye development	12	0.00000	E(spl) pp HLHm5 , HLHm5 pp HLHmdelta , HLHm3 pp HLHmbeta , HLHm3 pp HLHm5 , E(spl) pp HLHmdelta , HLHm7 pp HLHmdelta , HLHm5 pp HLHmbeta , HLHm5 pp HLHm7 , E(spl) pp HLHmbeta , HLHmbeta pp HLHmdelta , HLHm7 pp HLHmbeta , E(spl) pp HLHm7
6270	DNA replication initiation	5	0.00079	Mcm5 pp Mcm6 , Mcm3 pp Mcm6 , Mcm5 pp CDC45L , Mcm2 pp Mcm7 , Mcm2 pp dpa

7219	Notch signaling pathway	5	0.00328	E(spl) pp HLHmbeta , HLHm3 pp HLHmbeta , numb pp N , HLHmbeta pp HLHmdelta , E(spl) pp HLHmdelta
86	G2/M transition of mitotic cell cycle	2	0.00499	CycB pp cdc2 , CycA pp cdc2
6267	pre-replicative complex assembly	3	0.01359	Mcm5 pp Mcm6 , Mcm3 pp Mcm6 , Mcm2 pp Mcm7
6355	regulation of transcription, DNA-dependent	11	0.03505	ase pp HLHm7 , E(spl) pp HLHm5 , ase pp HLHm3 , Myb pp Dp , HLHm3 pp HLHm5 , Dll pp nej , ttk pp Stat92E , HLHm5 pp HLHm7 , HLHm7 pp sc , Lim1 pp CG11696 , E(spl) pp HLHm7
9987	cellular process	4	0.04864	CycB pp cdc2 , Prosalpha5 pp Pros25 , CycA pp cdc2 , CG17331 pp Pros25
7399	nervous system development	5	0.04881	HLHm5 pp HLHmbeta , HLHm5 pp HLHmdelta , ac pp HLHmbeta , arm pp shg , HLHmbeta pp HLHmdelta

Table S.5 Functional modules of MCC network in stage 5 (window size = 12).

GOID	Function name	#Edges	P-value	Edges
6511	ubiquitin-dependent protein catabolic process	20	1.76E-09	Prosbeta3 pp Prosbeta5 , Pros26.4 pp Pros35 , Prosalpha6T pp CG17331 , Prosbeta5R pp Pros35 , Prosalpha6T pp Pros25 , Prosbeta5 pp Pros25 , CG17331 pp Pros35 , Prosbeta5R pp Pros25 , Prosbeta3 pp Pros35 , Prosalpha7 pp Prosalpha6T , Prosbeta3 pp Prosalpha6T , Prosalpha7 pp Prosbeta3 , Prosbeta2 pp CG17331 , Prosalpha6T pp Prosbeta5R , CG17331 pp Pros25 , Prosbeta5 pp Pros35 , Prosalpha5 pp Pros25 , Prosalpha7 pp Pros35 , Pros26.4 pp Pros54 , Prosbeta3 pp CG17331
48749	compound eye development	9	0.00039	E(spl) pp HLHm5 , HLHm5 pp HLHmdelta , HLHm3 pp HLHmbeta , HLHm3 pp HLHm5 , E(spl) pp HLHmdelta , E(spl) pp HLHmbeta , HLHmbeta pp HLHmdelta , HLHm7 pp HLHmbeta , E(spl) pp HLHm7
6270	DNA replication initiation	4	0.00754	Mcm5 pp Mcm6 , Mcm3 pp Mcm6 , Mcm2 pp Mcm7 , Mcm2 pp dpa
6267	pre-replicative complex assembly	3	0.01488	Mcm5 pp Mcm6 , Mcm3 pp Mcm6 , Mcm2 pp Mcm7

Table S.6 Functional modules of MCC network in stage 6 (window size = 12).

GOID	Function name	#Edges	P-value	Edges
6511	ubiquitin-dependent protein catabolic process	18	1.72E-08	Prosbeta3 pp Prosbeta5 , Prosalpha7 pp Pros25 , Pros26.4 pp Pros35 , Prosalpha6T pp CG17331 , Prosbeta5R pp Pros35 , Prosalpha6T pp Pros25 , Prosbeta5R pp Pros25 , RpS27A pp Pros54 , Prosbeta3 pp Pros35 , Prosalpha7 pp Prosalpha6T , Prosbeta3 pp Prosalpha6T , Prosalpha7 pp Prosbeta3 , Prosbeta2 pp CG17331 , Prosalpha6T pp Prosbeta5R , CG17331 pp Pros25 , Prosbeta5 pp Pros35 , Prosalpha7 pp Pros35 , Prosbeta3 pp CG17331
45451	pole plasm oskar mRNA localization	2	0.01240	Hrb27C pp sqd , mago pp tsu
48749	compound eye development	6	0.01634	E(spl) pp HLHm5 , HLHm5 pp HLHmdelta , HLHm3 pp HLHm5 , HLHmbeta pp HLHmgamma , E(spl) pp HLHmdelta , E(spl) pp HLHm7
6355	regulation of transcription, DNA-dependent	10	0.04876	ase pp HLHm7 , E(spl) pp HLHm5 , Lim3 pp tup , ase pp HLHm3 , Myb pp Dp , HLHm3 pp HLHm5 , ac pp HLHm7 , HLHm7 pp sc , Lim1 pp CG11696 , E(spl) pp HLHm7

Table S.7 Functional modules of MCC network in stage 7 (window size = 12).

GOID	Function name	#Edges	P-value	Edges
6511	ubiquitin-dependent protein catabolic process	14	2.89E-06	Prosbeta3 pp Prosbeta5 , Prosbeta3 pp Pros35 , Pros26.4 pp Pros35 , Prosalpha7 pp Prosalpha6T , Prosalpha6T pp CG17331 , Prosbeta3 pp Prosalpha6T , Prosalpha7 pp Prosbeta3 , Prosbeta2 pp CG17331 , Prosalpha6T pp Prosbeta5R , CG17331 pp Pros25 , Prosalpha6T pp Pros25 , Prosbeta5 pp Pros35 , Prosalpha7 pp Pros35 , Prosbeta5R pp Pros25
45451	pole plasm oskar mRNA localization	2	0.00907	Hrb27C pp sqd , mago pp tsu
30718	germ-line stem cell maintenance	2	0.01714	Gef26 pp Rap2l , Dl pp N
6270	DNA replication initiation	3	0.02350	Mcm5 pp Mcm6 , Mcm2 pp Mcm7 , Mcm2 pp dpa
7498	mesoderm development	2	0.02698	eya pp pcs , Dl pp N
7219	Notch signaling pathway	3	0.04769	numb pp N , HLHmbeta pp HLHmgamma , Dl pp N

Table S.8 Functional modules of MCC network in stage 8 (window size = 12).

GOID	Function name	#Edges	P-value	Edges
6511	ubiquitin-dependent protein catabolic process	13	0.00001	Prosbeta3 pp Prosbeta5 , Prosbeta3 pp Pros35 , Pros26.4 pp Pros35 , Prosalpha7 pp Prosalpha6T , Prosalpha6T pp CG17331 , Prosbeta3 pp Prosalpha6T , Prosalpha7 pp Prosbeta3 , Prosalpha6T pp Prosbeta5R , CG17331 pp Prosbeta7 , CG17331 pp Pros25 , Pros28.1 pp Prosbeta5 , Prosbeta5 pp Pros35 , Prosalpha7 pp Pros35
6267	pre-replicative complex assembly	4	0.00049	Mcm5 pp Mcm6 , Mcm3 pp Mcm6 , Mcm2 pp Mcm10 , Mcm2 pp Mcm7
6270	DNA replication initiation	4	0.00277	Mcm5 pp Mcm6 , Mcm3 pp Mcm6 , Mcm2 pp Mcm7 , Mcm2 pp dpa
7219	Notch signaling pathway	4	0.00820	numb pp N , E(spl) pp HLHmgamma , HLHmbeta pp HLHmgamma , Dl pp N
45451	pole plasm oskar mRNA localization	2	0.00857	Hrb27C pp sqd , mago pp tsu
30718	germ-line stem cell maintenance	2	0.01621	Gef26 pp Rap2l , Dl pp N
7424	open tracheal system development	3	0.01730	sinu pp stumps , Btk29A pp sty , Dl pp N
9987	cellular process	4	0.02379	CycB pp cdc2 , Mov34 pp Rpn12 , CG17331 pp Prosbeta7 , CG17331 pp Pros25
16360	sensory organ precursor cell fate determination	2	0.02556	numb pp N , neur pp Tom
48749	compound eye development	5	0.02652	HLHm3 pp HLHm5 , E(spl) pp HLHmgamma , HLHmbeta pp HLHmgamma , E(spl) pp HLHm7 , Dl pp N

GOID	Function name	#Edges	P-value	Edges
6260	DNA replication	3	0.04461	DNApol-alpha73 pp DNApol-alpha180 , Mcm2 pp Mcm10 , Mcm2 pp dpa

Table S.9 Functional modules of MCC network in stage 9 (window size = 12).

GOID	Function name	#Edges	P-value	Edges
6270	DNA replication initiation	5	0.00042	Mcm5 pp Mcm6 , dpa pp Mcm6 , Mcm3 pp Mcm6 , Mcm2 pp Mcm7 , Mcm2 pp dpa
6267	pre-replicative complex assembly	4	0.00075	Mcm5 pp Mcm6 , Mcm3 pp Mcm6 , Mcm2 pp Mcm10 , Mcm2 pp Mcm7
7424	open tracheal system development	4	0.00294	sinu pp stumps , Btk29A pp sty , Dl pp N , Rac1 pp Rac2
86	G2/M transition of mitotic cell cycle	2	0.00379	CycB pp cdc2 , CycA pp cdc2
8347	glial cell migration	2	0.00379	numb pp N , Dl pp N
9987	cellular process	5	0.00759	CycB pp cdc2 , Mov34 pp Rpn12 , CycA pp cdc2 , CycA pp CycE , CG17331 pp Pros25
6260	DNA replication	4	0.01194	dpa pp Mcm6 , DNApol-alpha73 pp DNApol-alpha180 , Mcm2 pp Mcm10 , Mcm2 pp dpa
7219	Notch signaling pathway	4	0.01194	numb pp N , E(spl) pp HLHmgamma , HLHmbeta pp HLHmgamma , Dl pp N
30718	germ-line stem cell maintenance	2	0.02006	Gef26 pp Rap2l , Dl pp N
6511	ubiquitin-dependent protein catabolic process	8	0.02144	Prosbeta3 pp Pros35 , Pros26.4 pp Pros35 , Prosalpha7 pp Prosalpha6T , Prosalpha6T pp CG17331 , Prosbeta3 pp Prosalpha6T , Prosalpha6T pp Prosbeta5R , CG17331 pp Pros25 , lin19 pp skpA
16360	sensory organ precursor cell fate determination	2	0.03142	numb pp N , neur pp Tom

Table S.10   Functional modules of MCC network in stage 10 (window size = 12).

GOID	Function name	#Edges	P-value	Edges
6267	pre-replicative complex assembly	7	5.86E-08	Mcm5 pp Mcm6 , Mcm3 pp Mcm6 , Mcm5 pp Mcm3 , Mcm2 pp Mcm3 , Mcm2 pp Mcm10 , Mcm2 pp Mcm7 , Mcm2 pp Mcm5
6270	DNA replication initiation	8	1.97E-07	Mcm5 pp Mcm6 , dpa pp Mcm6 , Mcm3 pp Mcm6 , Mcm5 pp Mcm3 , Mcm2 pp Mcm3 , Mcm2 pp Mcm7 , Mcm2 pp Mcm5 , Mcm2 pp dpa
86	G2/M transition of mitotic cell cycle	2	0.00511	CycB pp cdc2 , CycA pp cdc2
8347	glial cell migration	`	0.00511	numb pp N , Dl pp N
6334	nucleosome assembly	3	0.00941	His3.3B pp asf1 , His3.3A pp asf1 , Iswi pp Acf1
9987	cellular process	5	0.01354	CycB pp cdc2 , CycA pp cdc2 , cdc2c pp Pros26.4 , CycA pp CycE , cdc2 pp CycE
30718	germ-line stem cell maintenance	2	0.02648	Gef26 pp Rap2l , Dl pp N
7424	open tracheal system development	3	0.03322	Btk29A pp sty , Dl pp N , Rac1 pp Rac2

Table S.11 Functional modules of MCC network in stage 11 (window size = 12).

GOID	Function name	#Edges	P-value	Edges
6267	pre-replicative complex assembly	7	1.37E-07	Mcm5 pp Mcm6 , Mcm3 pp Mcm6 , Mcm5 pp Mcm3 , Mcm2 pp Mcm3 , Mcm2 pp Mcm10 , Mcm2 pp Mcm7 , Mcm2 pp Mcm5
6270	DNA replication initiation	8	5.09E-07	Mcm5 pp Mcm6 , dpa pp Mcm6 , Mcm3 pp Mcm6 , Mcm5 pp Mcm3 , Mcm2 pp Mcm3 , Mcm2 pp Mcm7 , Mcm2 pp Mcm5 , Mcm2 pp dpa
7307	eggshell chorion gene amplification	6	0.00039	Myb pp Rbf , Myb pp Dp , Rbf pp mip130 , Dp pp Caf1 , Myb pp mip130 , Dp pp mip130
86	G2/M transition of mitotic cell cycle	2	0.00649	CycB pp cdc2 , CycA pp cdc2
8347	glial cell migration	2	0.00649	numb pp N , Dl pp N
16584	nucleosome positioning	2	0.00649	Iswi pp Caf1 , Iswi pp Acf1
48749	compound eye development	7	0.01168	HLHm5 pp HLHmbeta , E(spl) pp HLHmbeta , ey pp tsr , HLHm7 pp HLHmbeta , E(spl) pp HLHmdelta , Dl pp N , HLHm7 pp HLHmgamma
7517	muscle development	5	0.01185	esc pp E(z) , esc pp Caf1 , Iswi pp Caf1 , Dp pp Caf1 , Iswi pp Acf1
6334	nucleosome assembly	3	0.01299	His3.3B pp asf1 , Iswi pp Caf1 , Iswi pp Acf1
6342	chromatin silencing	5	0.01763	esc pp E(z) , Su(var)3-9 pp Rpd3 , E(z) pp corto , esc pp Caf1 , esc pp corto
51297	centrosome organization	2	0.01792	Prosbeta5 pp Prosbeta7 , Myb pp mip130
6260	DNA replication	4	0.02774	dpa pp Mcm6 , DNApol-alpha73 pp DNApol-alpha180 , Mcm2 pp Mcm10 , Mcm2 pp dpa

7219	Notch signaling pathway	4	0.02774	E(spl) pp HLHmbeta , numb pp N , E(spl) pp HLHmdelta , Dl pp N
30718	germ-line stem cell maintenance	2	0.03299	Gef26 pp Rap2l , Dl pp N
16571	histone methylation	3	0.04405	esc pp E(z) , Su(var)3-9 pp Rpd3 , esc pp Caf1

Table S.12 Functional modules of MCC network in stage 12 (window size = 12).

GOID	Function name	#Edges	P-value	Edges
6267	pre-replicative complex assembly	8	4.91E-09	Mcm5 pp Mcm6 , Mcm3 pp Mcm6 , Mcm5 pp Mcm3 , Mcm2 pp Mcm3 , Mcm2 pp Mcm10 , Mcm2 pp Mcm7 , Mcm2 pp Mcm6 , Mcm2 pp Mcm5
6270	DNA replication initiation	8	1.68E-06	Mcm5 pp Mcm6 , Mcm3 pp Mcm6 , Mcm5 pp Mcm3 , Mcm2 pp Mcm3 , Mcm2 pp Mcm7 , Mcm2 pp dpa , Mcm2 pp Mcm6 , Mcm2 pp Mcm5
7307	eggshell chorion gene amplification	7	0.00010	Myb pp Rbf , Myb pp Dp , Rbf pp mip130 , dup pp geminin , Dp pp Caf1 , Myb pp mip130 , Dp pp mip130
7517	muscle development	7	0.00091	Caf1 pp Su(z)12 , Caf1 pp Rpd3 , esc pp E(z) , esc pp Caf1 , Iswi pp Caf1 , Dp pp Caf1 , Iswi pp Acf1
6342	chromatin silencing	7	0.00173	Caf1 pp Su(z)12 , Caf1 pp Rpd3 , esc pp E(z) , Su(var)3-9 pp Rpd3 , E(z) pp corto , esc pp Caf1 , esc pp corto
16571	histone methylation	5	0.00178	Caf1 pp Su(z)12 , Caf1 pp Rpd3 , esc pp E(z) , Su(var)3-9 pp Rpd3 , esc pp Caf1
48749	compound eye development	9	0.00225	E(spl) pp HLHm5 , HLHm5 pp HLHmdelta , E(spl) pp HLHmdelta , HLHm7 pp HLHmgamma , HLHm3 pp HLHmdelta , HLHm5 pp HLHmbeta , E(spl) pp HLHmbeta , HLHm7 pp HLHmbeta , Dl pp N
86	G2/M transition of mitotic cell cycle	2	0.00879	CycB pp cdc2 , CycA pp cdc2
16584	nucleosome positioning	2	0.00879	Iswi pp Caf1 , Iswi pp Acf1

6260	DNA replication	5	0.01046	DNApol-alpha73 pp DNApol-alpha50 , Mcm2 pp Mcm6 , DNApol-alpha73 pp DNApol-alpha180 , Mcm2 pp Mcm10 , Mcm2 pp dpa
122	negative regulation of transcription from RNA polymerase II promoter	8	0.01666	HLHmdelta pp CtBP , kni pp CtBP , E(spl) pp HLHmdelta , HLHm3 pp HLHmdelta , Rbf pp E2f2 , Rbf pp mip130 , E(spl) pp HLHmbeta , per pp tim
6334	nucleosome assembly	3	0.01938	His3.3B pp asf1 , Iswi pp Caf1 , Iswi pp Acf1
7096	regulation of exit from mitosis	2	0.02393	CycE pp ago , rux pp CycE
51297	centrosome organization	2	0.02393	Prosbeta5 pp Prosbeta7 , Myb pp mip130
48813	dendrite morphogenesis	7	0.03000	Caf1 pp Su(z)12 , Caf1 pp Rpd3 , esc pp E(z) , esc pp Caf1 , Iswi pp Caf1 , Dp pp Caf1 , Iswi pp Acf1
7219	Notch signaling pathway	4	0.04303	E(spl) pp HLHmbeta , E(spl) pp HLHmdelta , Dl pp N , HLHm3 pp HLHmdelta
6367	transcription initiation from RNA polymerase II promoter	7	0.04571	MED31 pp MED17 , Taf4 pp Taf1 , Taf10 pp Spt3 , TfIIEalpha pp TfIIEbeta , MED17 pp MED21 , Mat1 pp MED15 , MED6 pp MED17
48666	neuron development	3	0.04969	Caf1 pp Su(z)12 , esc pp Caf1 , Dp pp Caf1

Table S.13 Functional modules of MCC network in stage 13 (window size = 12).

GOID	Function name	#Edges	P-value	Edges
7307	eggshell chorion gene amplification	7	0.00018	Myb pp Rbf , Myb pp Dp , Rbf pp mip130 , dup pp geminin , Dp pp Caf1 , Myb pp mip130 , Dp pp mip130
6270	DNA replication initiation	5	0.00414	Mcm5 pp Mcm6 , Mcm5 pp CDC45L , Mcm2 pp Mcm7 , Mcm2 pp Mcm5 , Mcm2 pp dpa
6267	pre-replicative complex assembly	4	0.00498	Mcm5 pp Mcm6 , Mcm2 pp Mcm10 , Mcm2 pp Mcm7 , Mcm2 pp Mcm5
7517	muscle development	6	0.00756	Caf1 pp Su(z)12 , esc pp E(z) , esc pp Caf1 , Iswi pp Caf1 , Dp pp Caf1 , Iswi pp Acf1
30261	chromosome condensation	3	0.00870	Mcm5 pp CDC45L , Mcm2 pp Mcm10 , Mcm2 pp Mcm5
86	G2/M transition of mitotic cell cycle	2	0.01058	CycB pp cdc2 , CycA pp cdc2
16584	nucleosome positioning	2	0.01058	Iswi pp Caf1 , Iswi pp Acf1
48666	neuron development	4	0.01209	Caf1 pp Su(z)12 , esc pp Caf1 , Dp pp Caf1 , E(spl) pp HLHm7
6342	chromatin silencing	6	0.01225	Caf1 pp Su(z)12 , esc pp E(z) , Su(var)3-9 pp Rpd3 , E(z) pp corto , esc pp Caf1 , esc pp corto
48749	compound eye development	8	0.01293	E(spl) pp HLHm5 , E(spl) pp HLHmdelta , HLHm3 pp HLHmdelta , HLHm5 pp HLHmbeta , E(spl) pp HLHmbeta , HLHm7 pp HLHmbeta , Dl pp N , E(spl) pp HLHm7
16571	histone methylation	4	0.01709	Caf1 pp Su(z)12 , esc pp E(z) , Su(var)3-9 pp Rpd3 , esc pp Caf1

48813	dendrite morphogenesis	8	0.01748	Caf1 pp Su(z)12 , esc pp Caf1 , Iswi pp Caf1 , ci pp Bap55 , esc pp E(z) , Dp pp Caf1 , E(spl) pp HLHm7 , Iswi pp Acf1
6334	nucleosome assembly	3	0.02459	His3.3B pp asf1 , Iswi pp Caf1 , Iswi pp Acf1
6357	regulation of transcription from RNA polymerase II promoter	10	0.02581	MED31 pp MED17 , e(y)1 pp TfIIB , lolal pp bip2 , lola pp apt , Trl pp bip2 , skd pp CycC , MED6 pp MED17 , lola pp bip2 , MED17 pp MED22 , ttk pp bip2
122	negative regulation of transcription from RNA polymerase II promoter	8	0.02594	HLHmdelta pp CtBP , kni pp CtBP , E(spl) pp HLHmdelta , HLHm3 pp HLHmdelta , Rbf pp E2f2 , Rbf pp mip130 , E(spl) pp HLHmbeta , per pp tim
7096	regulation of exit from mitosis	2	0.02851	CycE pp ago , rux pp CycE
51297	centrosome organization	2	0.02851	Prosbeta5 pp Prosbeta7 , Myb pp mip130
82	G1/S transition of mitotic cell cycle	3	0.03536	cdc2 pp E2f , CycC pp dap , cdc2 pp CycC

Table S.14 Functional modules of MCC network in stage 14 (window size = 12).

GOID	Function name	#Edges	P-value	Edges
7307	eggshell chorion gene amplification	7	0.00020	Myb pp Rbf , Myb pp Dp , Rbf pp mip130 , dup pp geminin , Dp pp Caf1 , Myb pp mip130 , Dp pp mip130
48749	compound eye development	11	0.00031	E(spl) pp HLHm5 , HLHm3 pp HLHmbeta , E(spl) pp HLHmdelta , HLHm5 pp HLHmbeta , HLHm5 pp HLHm7 , E(spl) pp HLHmbeta , HLHm5 pp HLHmgamma , HLHmbeta pp HLHmdelta , HLHm7 pp HLHmbeta , Dl pp N , E(spl) pp HLHm7
82	G1/S transition of mitotic cell cycle	4	0.00528	cdc2 pp E2f , CycC pp dap , cdc2 pp CycC , cdc2 pp CycE
7517	muscle development	6	0.00813	Caf1 pp Su(z)12 , esc pp E(z) , esc pp Caf1 , Iswi pp Caf1 , Dp pp Caf1 , Iswi pp Acf1
30261	chromosome condensation	3	0.00909	Mcm5 pp CDC45L , Mcm2 pp Mcm10 , Mcm2 pp Mcm5
86	G2/M transition of mitotic cell cycle	2	0.01092	CycB pp cdc2 , CycA pp cdc2
16584	nucleosome positioning	2	0.01092	Iswi pp Caf1 , Iswi pp Acf1
8586	imaginal disc-derived wing vein morphogenesis	2	0.01092	Su(dx) pp Mad , sog pp tld
48666	neuron development	4	0.01275	Caf1 pp Su(z)12 , esc pp Caf1 , Dp pp Caf1 , E(spl) pp HLHm7
6342	chromatin silencing	6	0.01313	Caf1 pp Su(z)12 , esc pp E(z) , Su(var)3-9 pp Rpd3 , Asx pp ph-p , esc pp Caf1 , esc pp corto
7219	Notch signaling pathway	5	0.01588	E(spl) pp HLHmbeta , HLHm3 pp HLHmbeta , HLHmbeta pp HLHmdelta , E(spl) pp HLHmdelta , Dl pp N

16571	histone methylation	4	0.01799	Caf1 pp Su(z)12 , esc pp E(z) , Su(var)3-9 pp Rpd3 , , esc pp Caf1
6270	DNA replication initiation	4	0.02422	Mcm5 pp CDC45L , Mcm2 pp Mcm7 , Mcm2 pp Mcm5 , Mcm2 pp dpa
122	negative regulation of transcription from RNA polymerase II promoter	8	0.02790	HLHmdelta pp CtBP , E(spl) pp HLHmbeta , HLHm3 pp HLHmbeta , kni pp CtBP , Rbf pp mip130 , HLHmbeta pp HLHmdelta , E(spl) pp HLHmdelta , Rbf pp E2f2
6367	transcription initiation from RNA polymerase II promoter	8	0.03133	CycC pp CycH , Taf4 pp Taf1 , Taf10 pp Spt3 , e(y)1 pp TfIIB , skd pp CycC , Mat1 pp MED15 , MED6 pp MED17 , Taf11 pp Taf13
6267	pre-replicative complex assembly	3	0.03675	Mcm2 pp Mcm10 , Mcm2 pp Mcm7 , Mcm2 pp Mcm5
45893	positive regulation of transcription, DNA-dependent	3	0.03675	z pp Bap170 , mor pp z , z pp dalao
48813	dendrite morphogenesis	7	0.04590	Caf1 pp Su(z)12 , esc pp E(z) , esc pp Caf1 , Iswi pp Caf1 , Dp pp Caf1 , Iswi pp Acf1 , E(spl) pp HLHm7

Table S.15 Functional modules of MCC network in stage 15 (window size = 12).

GOID	Function name	#Edges	P-value	Edges
82	G1/S transition of mitotic cell cycle	5	0.00071	cdc2 pp E2f , CycC pp dap , cdc2 pp CycC , dap pp CycE , cdc2 pp CycE
30261	chromosome condensation	4	0.00072	Orc2 pp Mcm10 , Mcm2 pp Mcm10 , CDC45L pp Mcm10 , Mcm2 pp Mcm5
7307	eggshell chorion gene amplification	6	0.00235	Myb pp Rbf , Myb pp Dp , Rbf pp mip130 , Dp pp Rbf , Dp pp Caf1 , Dp pp mip130
6260	DNA replication	6	0.00496	dup pp Mcm10 , Mcm2 pp Mcm6 , Orc2 pp Mcm10 , Mcm2 pp Mcm10 , CDC45L pp Mcm10 , Mcm2 pp dpa
9987	cellular process	7	0.00652	CycB pp cdc2 , cdc2 pp E2f , CycA pp cdc2 , cdc2c pp Pros26.4 , cdc2 pp CycE , CycA pp E2f , CG17331 pp Pros25
6267	pre-replicative complex assembly	4	0.00709	Mcm2 pp Mcm6 , Mcm2 pp Mcm10 , Mcm2 pp Mcm7 , Mcm2 pp Mcm5
7517	muscle development	6	0.01183	Caf1 pp Su(z)12 , esc pp E(z) , esc pp Caf1 , Iswi pp Caf1 , Dp pp Caf1 , Iswi pp Acf1
86	G2/M transition of mitotic cell cycle	2	0.01290	CycB pp cdc2 , CycA pp cdc2
30177	positive regulation of Wnt receptor signaling pathway	2	0.01290	kto pp skd , lgs pp pygo
16584	nucleosome positioning	2	0.01290	Iswi pp Caf1 , Iswi pp Acf1
7423	sensory organ development	4	0.01679	emc pp sc , dap pp CycE , neur pp Tom , Dl pp N
48666	neuron development	4	0.01679	Caf1 pp Su(z)12 , esc pp Caf1 , Dp pp Caf1 , E(spl) pp HLHm7
16571	histone methylation	4	0.02343	Caf1 pp Su(z)12 , esc pp E(z) , Su(var)3-9 pp Rpd3 , esc pp Caf1

398	nuclear mRNA splicing, via spliceosome	7	0.03050	noi pp CG16941 , U2af50 pp U2af38 , CG6610 pp snRNP2 , CG3294 pp CG7757 , DebB pp snRNP2 , U2af50 pp CG7757 , pUf68 pp CG7757
6270	DNA replication initiation	4	0.03123	Mcm2 pp Mcm6 , Mcm2 pp Mcm7 , Mcm2 pp Mcm5 , Mcm2 pp dpa
7402	ganglion mother cell fate determination	2	0.03435	pros pp brat , brat pp mira
7113	endomitotic cell cycle	2	0.03435	Dp pp Rbf , Rbf pp E2f2
7049	cell cycle	4	0.04006	Myb pp Dp , cdc2 pp CycE , Sep1 pp Sep2 , cdc2 pp Cks30A
6511	ubiquitin-dependent protein catabolic process	11	0.04349	Prosbeta3 pp Prosbeta5 , Prosbeta3 pp Prosbeta5R , Prosalpha7 pp Prosalpha6T , Prosalpha6T pp CG17331 , CG17331 pp Pros25 , lin19 pp skpA , Elongin-C pp cul-2 , Prosbeta3 pp Pros25 , Prosbeta5 pp Prosbeta7 , Prosbeta5R pp Pros25 , Pros54 pp CG17331
6367	transcription initiation from RNA polymerase II promoter	8	0.04454	CycC pp CycH , Taf4 pp Taf1 , Taf10 pp Spt3 , e(y)1 pp TfIIB , skd pp CycC , Mat1 pp MED15 , MED6 pp MED17 , kto pp skd

Table S.16 Functional modules of MCC network in stage 16 (window size = 12).

GOID	Function name	#Edges	P-value	Edges
48749	compound eye development	11	0.00055	E(spl) pp HLHm5 , HLHm3 pp HLHm5 , rux pp dan , HLHm7 pp HLHmgamma , HLHm3 pp HLHmdelta , HLHm5 pp HLHm7 , ey pp tsr , HLHm7 pp HLHmbeta , E(spl) pp HLHm7 , Dl pp N , Dl pp danr
6357	regulation of transcription from RNA polymerase II promoter	13	0.00321	MED31 pp MED17 , e(y)1 pp TfIIB , TfIIB pp Trf , MED17 pp MED28 , trh pp tgo , kto pp skd , apt pp bip2 , Trl pp lolal , skd pp CycC , Trl pp bip2 , MED6 pp MED17 , kto pp CycC , MED20 pp MED28
6270	DNA replication initiation	5	0.00591	dpa pp Mcm5 , Mcm2 pp Mcm6 , Mcm2 pp Mcm7 , Mcm2 pp Mcm5 , Mcm2 pp dpa
9987	cellular process	7	0.00604	CycB pp cdc2 , cdc2 pp E2f , CycA pp cdc2 , cdc2c pp Pros26.4 , cdc2 pp CycE , CycA pp E2f , CG17331 pp Pros25
6267	pre-replicative complex assembly	4	0.00673	Mcm2 pp Mcm6 , Mcm2 pp Mcm10 , Mcm2 pp Mcm7 , Mcm2 pp Mcm5
82	G1/S transition of mitotic cell cycle	4	0.00673	cdc2 pp E2f , CycC pp dap , cdc2 pp CycC , cdc2 pp CycE
6367	transcription initiation from RNA polymerase II promoter	10	0.00689	MED31 pp MED17 , e(y)1 pp TfIIB , TfIIB pp Trf , kto pp skd , Taf11 pp Taf13 , Taf10 pp Spt3 , skd pp CycC , Mat1 pp MED15 , MED6 pp MED17 , kto pp CycC
30261	chromosome condensation	3	0.01100	Orc2 pp Mcm10 , Mcm2 pp Mcm10 , Mcm2 pp Mcm5

86	G2/M transition of mitotic cell cycle	2	0.01253	CycB pp cdc2 , CycA pp cdc2
30177	positive regulation of Wnt receptor signaling pathway	2	0.01253	kto pp skd , lgs pp pygo
16584	nucleosome positioning	2	0.01253	Iswi pp Caf1 , Iswi pp Acf1
7015	actin filament organization	3	0.03046	Dl pp Fs(2)Ket , ena pp drk , Dl pp N
7402	ganglion mother cell fate determination	2	0.03342	pros pp brat , brat pp mira
45893	positive regulation of transcription, DNA-dependent	3	0.04336	mor pp dalao , mor pp z , z pp dalao
7307	eggshell chorion gene amplification	4	0.04785	Myb pp Rbf , Myb pp Dp , Rbf pp mip130 , Dp pp mip130

Table S.17 Functional modules of MCC network in stage 17 (window size = 12).

GOID	Function name	#Edges	P-value	Edges
6267	pre-replicative complex assembly	5	0.00060	Mcm2 pp Mcm6 , Mcm5 pp Mcm3 , Mcm2 pp Mcm10 , Mcm2 pp Mcm7 , Mcm2 pp Mcm5
30261	chromosome condensation	4	0.00062	Orc2 pp Mcm10 , Mcm2 pp Mcm10 , CDC45L pp Mcm10 , Mcm2 pp Mcm5
6270	DNA replication initiation	6	0.00075	dpa pp Mcm5 , Mcm2 pp Mcm6 , Mcm5 pp Mcm3 , Mcm2 pp Mcm7 , Mcm2 pp Mcm5 , Mcm2 pp dpa
48749	compound eye development	10	0.00179	E(spl) pp HLHm5 , HLHm5 pp HLHmdelta , HLHm3 pp HLHm5 , rux pp dan , HLHm7 pp HLHmdelta , HLHm5 pp HLHm7 , HLHmbeta pp HLHmdelta , Dl pp N , Dl pp danr , E(spl) pp HLHm7
6260	DNA replication	6	0.00415	Mcm2 pp Mcm6 , CG8142 pp RfC3 , Orc2 pp Mcm10 , Mcm2 pp Mcm10 , CDC45L pp Mcm10 , Mcm2 pp dpa
9987	cellular process	7	0.00537	CycB pp cdc2 , cdc2 pp E2f , CycA pp cdc2 , cdc2c pp Pros26.4 , CycA pp E2f , Pros25 pp Prosbeta7 , CG17331 pp Pros25
7254	JNK cascade	4	0.00622	Rac1 pp Pak , Pak pp Rac2 , bsk pp Aplip1 , Rac1 pp Rac2

6511	ubiquitin-dependent protein catabolic process	13	0.00829	Prosbeta3 pp Prosbeta5 , Prosbeta5R pp Prosbeta7 , Prosbeta3 pp Prosbeta5R , Prosbeta3 pp Pros35 , Prosalpha7 pp Prosalpha6T , Prosalpha6T pp CG17331 , Pros25 pp Pros35 , RpL40 pp RpS27A , CG17331 pp Pros25 , Elongin-C pp cul-2 , Prosbeta5 pp Pros25 , Prosbeta5R pp Pros25 , Pros25 pp Prosbeta7
86	G2/M transition of mitotic cell cycle	2	0.01198	CycB pp cdc2 , CycA pp cdc2
30177	positive regulation of Wnt receptor signaling pathway	2	0.01198	kto pp skd , lgs pp pygo
16584	nucleosome positioning	2	0.01198	Iswi pp Caf1 , Iswi pp Acf1
8360	regulation of cell shape	4	0.01487	Abl pp ena , Hem pp Abi , ena pp drk , Cdc42 pp par-6
6334	nucleosome assembly	3	0.02880	E(bx) pp Iswi , Iswi pp Caf1 , Iswi pp Acf1
6468	protein amino acid phosphorylation	1	0.03064	bsk pp Cdk4
7402	ganglion mother cell fate determination	2	0.03205	pros pp brat , brat pp mira
6357	regulation of transcription from RNA polymerase II promoter	10	0.03523	e(y)1 pp TfIIB , TfIIB pp Trf , MED17 pp MED28 , kto pp skd , apt pp bip2 , Trl pp lolal , Trl pp bip2 , TfIIA-L pp TfIIA-S-2 , ttk pp lolal , MED20 pp MED28
6367	transcription initiation from RNA polymerase II promoter	8	0.03825	Taf4 pp Taf1 , Taf10 pp Spt3 , e(y)1 pp TfIIB , TfIIB pp Trf , Mat1 pp MED15 , TfIIA-L pp TfIIA-S-2 , kto pp skd , Taf11 pp Taf13
82	G1/S transition of mitotic cell cycle	3	0.04110	cdc2 pp E2f , CycC pp dap , cdc2 pp CycC

Table S.18   Functional modules of MCC network in stage 18 (window size = 12).

GOID	Function name	#Edges	P-value	Edges
6511	ubiquitin-dependent protein catabolic process	16	0.00039	Prosbeta3 pp Prosbeta5 , Prosalpha6T pp CG17331 , Pros25 pp Pros35 , RpL40 pp RpS27A , Elongin-C pp cul-2 , Prosbeta5 pp Pros25 , Prosbeta5R pp Pros25 , Pros25 pp Prosbeta7 , Prosbeta3 pp Pros35 , Prosbeta3 pp Prosbeta5R , Prosalpha7 pp Prosalpha6T , Prosbeta3 pp Prosalpha6T , Prosalpha7 pp Prosbeta3 , CG17331 pp Pros25 , Prosalpha7 pp CG17331 , Prosbeta5 pp CG17331
30261	chromosome condensation	4	0.00061	Orc2 pp Mcm10 , Mcm2 pp Mcm10 , CDC45L pp Mcm10 , Mcm2 pp Mcm5
6260	DNA replication	7	0.00067	dup pp Mcm10 , Mcm2 pp Mcm6 , CG8142 pp RfC3 , Orc2 pp Mcm10 , Mcm2 pp Mcm10 , CDC45L pp Mcm10 , Mcm2 pp dpa
6270	DNA replication initiation	5	0.00521	dpa pp Mcm5 , Mcm2 pp Mcm6 , Mcm2 pp Mcm7 , Mcm2 pp Mcm5 , Mcm2 pp dpa
6267	pre-replicative complex assembly	4	0.00605	Mcm2 pp Mcm6 , Mcm2 pp Mcm10 , Mcm2 pp Mcm7 , Mcm2 pp Mcm5
16584	nucleosome positioning	2	0.01180	Iswi pp Caf1 , Iswi pp Acf1
9987	cellular process	6	0.01906	CycB pp cdc2 , cdc2 pp E2f , CycA pp cdc2 , CycA pp E2f , Pros25 pp Prosbeta7 , CG17331 pp Pros25
7015	actin filament organization	3	0.02825	chic pp ena , ena pp drk , Dl pp N
7402	ganglion mother cell fate determination	2	0.03160	pros pp brat , brat pp mira
6468	protein amino acid	1	0.03167	bsk pp Cdk4

phosphorylation

7517	muscle development	5	0.03487	esc pp Rpd3 , Rpd3 pp Su(z)12 , Iswi pp Caf1 , E(z) pp Su(z)12 , Iswi pp Acf1
6911	phagocytosis, engulfment	5	0.04155	pros pp brat , Chi pp CG4328 , Cdc42 pp par-6 , cyp33 pp deltaCOP , Rac1 pp Rac2
6342	chromatin silencing	5	0.04871	esc pp Rpd3 , Rpd3 pp Su(z)12 , Su(var)3-9 pp Su(var)205 , E(z) pp Su(z)12 , esc pp corto